UNIVERSITY PARDUBICE,
Faculty of Chemical Technology, Department of Analytical Chemistry,
University of Pardubice, Studentská 573, **532 10 Pardubice,** Czech Republic,
(Prof. Ing. Karel Ventura, CSc.)

Telefon: *4240-603 1111 (centrála),
*4240-603 7026 (Meloun),
Fax: *4240-603 7068
E-mail: milan.meloun@upce.cz
http://meloun.upce.cz Prof. RNDr. Milan Meloun, DrSc.

01. 03. 2018

Dear Editor-in-Chief,

enclosed I send you the manuscript and figures of our paper

Multiple Dissociation Constants of the Intepirdine Using Regression of Multiwavelength Spectrophotometric pH-Titration Data

[*]Milan Meloun[1], Lucie Pilařová[1], Filip Bureš[2] and Tomáš Pekárek[3]
[1]Department of Analytical Chemistry, University of Pardubice, CZ 532 10 Pardubice, Czech Republic,
[2]Institute of Organic Chemistry and Technology, University of Pardubice, CZ 532 10 Pardubice, Czech Republic,
[3]Zentiva k.s., U kabelovny 130, CZ 102 37 Prague, Czech Republic
***Corresponding author:** milan.meloun@upce.cz, **Phone:** +420466037026, **Fax:** +420466037068

A statement that the paper is appropriate: This manuscript has not been previously published in any language anywhere and it is not under consideration by another journal. To date, no spectra, no dissociation constants or no pH-distribution diagrams of the relative concentration of variously protonated ions of the drug Intepirdine hydrochloride INN.HCl have been published.

1) **Significance of the work:** Medicine and pharmacology needs physical constants (spectra, pK´s, solubility, etc.) of new drugs.
2) **Novelty of the work:** INN.HCl is used for the treatment of mild to moderate Alzheimer's disease and dementia with Lewy bodies. Acid-base equilibria were studied with UV-metric spectra analysis and pH-metric titration analysis. Three pK^{T}_{a1}, pK^{T}_{a2}, pK^{T}_{a3}, of INN.HCl were determined at 25ºC and 37ºC in an aqueous medium. The number of variously protonated species was estimated from the rank of the UV-absorbance matrix.
3) **Contribution to the field:** Knowledge of the possible ionization states of a pharmaceutical substance, embodied in pK_a, is vital for understanding properties essential to drug development.

Yours sincerely

Prof. RNDr. Milan Meloun, DrSc.

Highlights:

- Acid-base equilibria were studied with UV-metric spectra analysis and pH-metric titration analysis.
- Three pK^{T}_{a1}, pK^{T}_{a2}, pK^{T}_{a3}, of INN.HCl were determined at 25ºC and 37ºC in an aqueous medium.
- The number of variously protonated species was estimated from the rank of the UV-absorbance matrix.
- The $\square_{LH3}$ and $\square_{LH4}$ show that protonation of chromophore LH_2^+ to LH_3^{2+} and LH_4^{3+} has less influence on chromophores in Intepirdine hydrochloride molecule than $\square_{LH}$ and $\square_{LH2}$.

Protonation of Intepirdine for the Treatment of Alzheimer´s disease

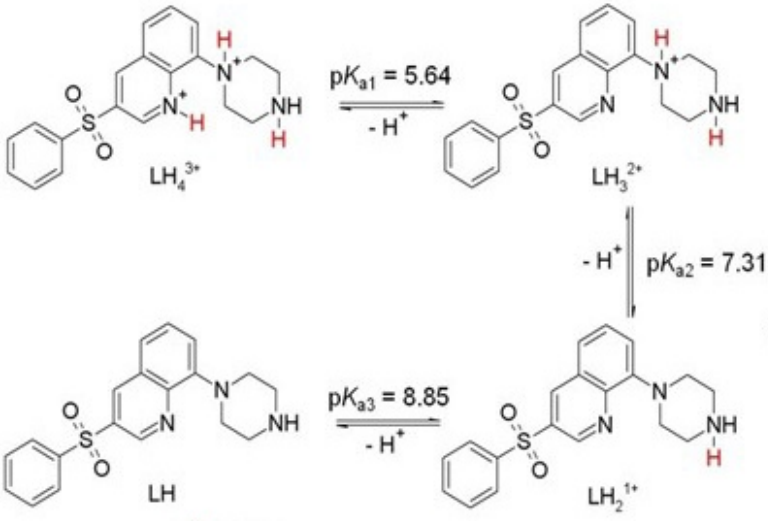

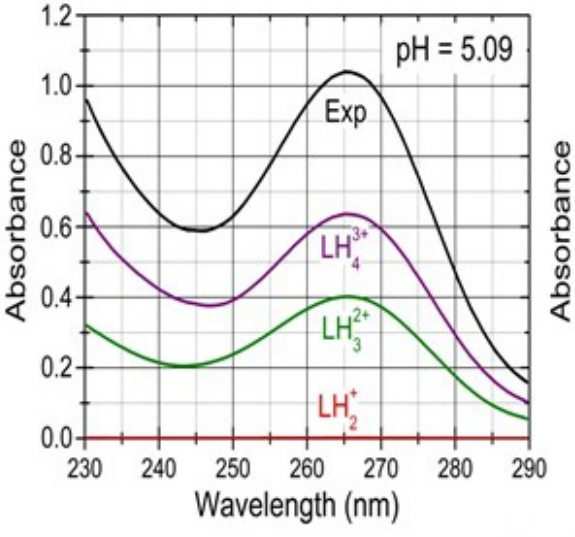

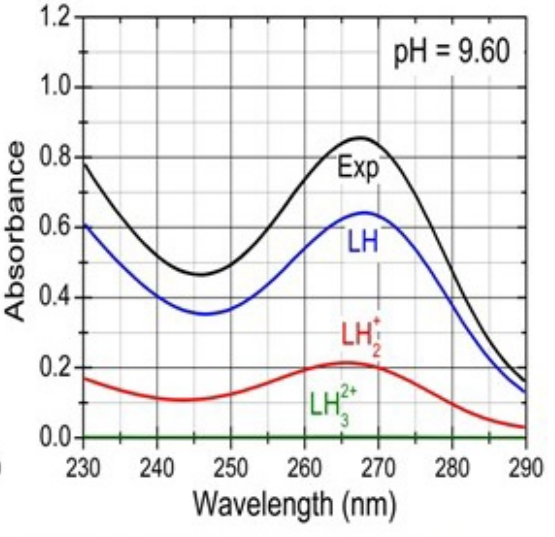

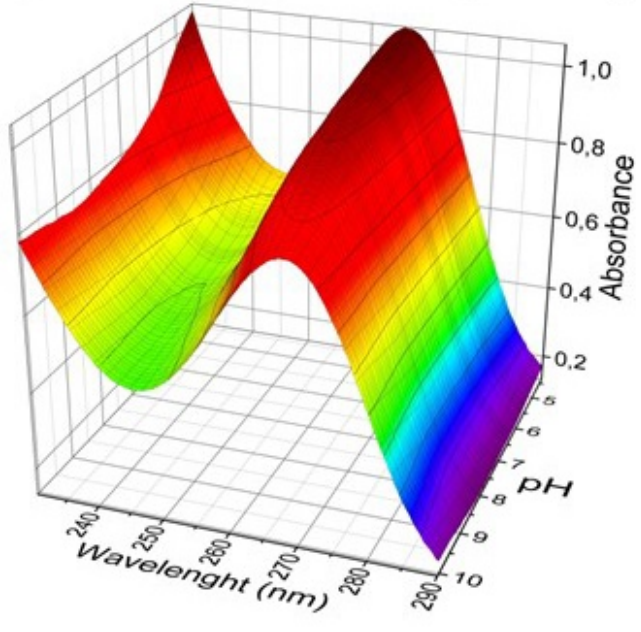

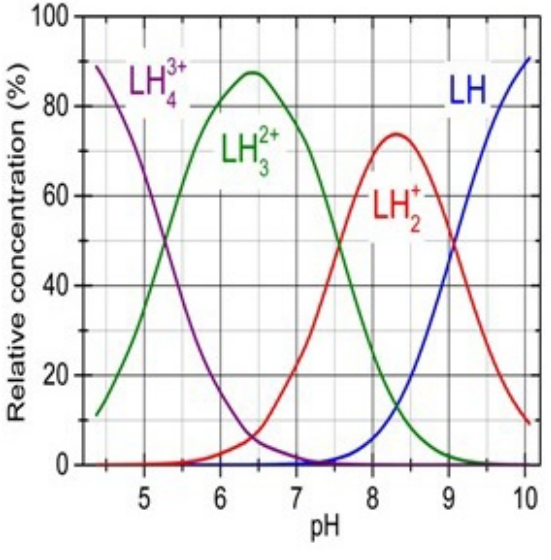

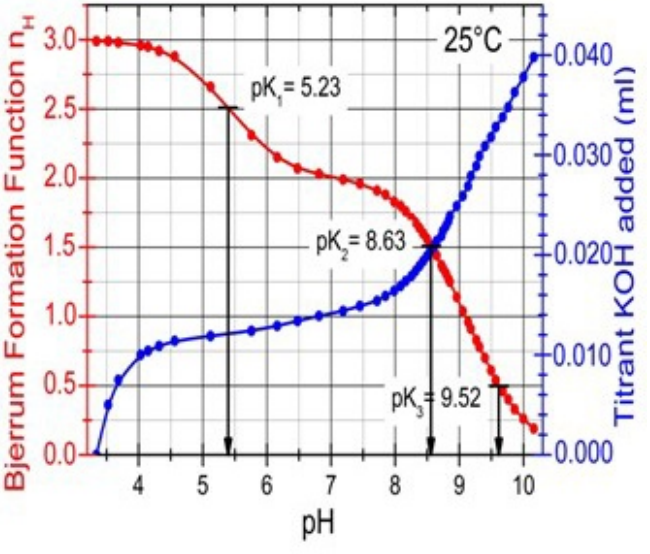

Multiple Dissociation Constants of the Intepirdine Hydrochloride Using Regression of Multiwavelength Spectrophotometric pH-Titration Data

[*]Milan Meloun[1], Lucie Pilařová[1], Filip Bureš[2] and Tomáš Pekárek[3]

[1]Department of Analytical Chemistry, University of Pardubice, CZ 532 10 Pardubice, Czech Republic,

[2]Institute of Organic Chemistry and Technology, University of Pardubice, CZ 532 10 Pardubice, Czech Republic,

[3]Zentiva k.s., U kabelovny 130, CZ 102 37 Prague, Czech Republic

***Corresponding author:** milan.meloun@upce.cz, **Phone:** +420466037026, **Fax:** +420466037068,

Abstract: Spectrophotometric and potentiometric pH-titrations of the Neurotransmitter Intepirdine hydrochloride INN.HCl for three dissociation constants determination were compared. A nonlinear regression of the pH-spectra (REACTLAB, SQUAD84) and of the pH-titration curve (ESAB) determined three multiple dissociation constants. A sparingly soluble neutral molecule LH of INN.HCl was capable of protonation to form the still soluble three cations LH_2^+, LH_3^{2+} and LH_4^{3+} in pure water. Although the change of pH somewhat less affected changes in the chromophore, three consecutive thermodynamic dissociation constants were estimated $pK^T_{a1} = 5.64$, $pK^T_{a2} = 7.31$, $pK^T_{a3} = 8.85$ at 25°C and $pK^T_{a1} = 5.51$, $pK^T_{a2} = 7.15$, $pK^T_{a3} = 8.77$ at 37°C. The graph of molar absorption coefficients of variously protonated species according to wavelength shows that the spectrum of species LH_2^+ and LH vary in colour, while protonation of chromophore LH_2^+ to LH_3^{2+} and LH_4^{3+} has less influence on chromophores in Intepirdine hydrochloride molecule. As the spectral response on the chromophore in the INN.HCl molecule is not large, it was necessary to test a reliability whether it is possible to estimate the dissociation constants even from such small spectrum changes. Three multiple thermodynamic dissociation constants of 3×10^{-4} M INN.HCl were determined by the regression analysis of potentiometric titration curves $pK^T_{a1} = 5.14$, $pK^T_{a2} = 8.38$, $pK^T_{a3} = 9.33$ at 25°C and $pK^T_{a1} = 5.17$, $pK^T_{a2} = 8.31$, $pK^T_{a3} = 9.07$ at 37°C. The macro-dissociation constants of INN.HCl were estimated according to the chemical structure analysed by two pK_a predictors, the MARVIN and ACD/Percepta programs. The resulting protonation scheme of INN.HCl was suggested.

Keywords Dissociation constants; Intepirdine hydrochloride; spectrophotometric titration; REACTLAB; SQUAD84; ESAB;

Highlights:

- Acid-base equilibria were studied with UV-metric spectra analysis and pH-metric titration analysis.
- Three pK^T_{a1}, pK^T_{a2}, pK^T_{a3}, of INN.HCl were determined at 25ºC and 37ºC in an aqueous medium.
- The number of variously protonated species was estimated from the rank of the UV-absorbance matrix.
- The ε_{LH3} and ε_{LH4} show that protonation of chromophore LH_2^+ to LH_3^{2+} and LH_4^{3+} has less influence on chromophores in Intepirdine hydrochloride molecule than ε_{LH} and ε_{LH2}.

Graphical abstract:

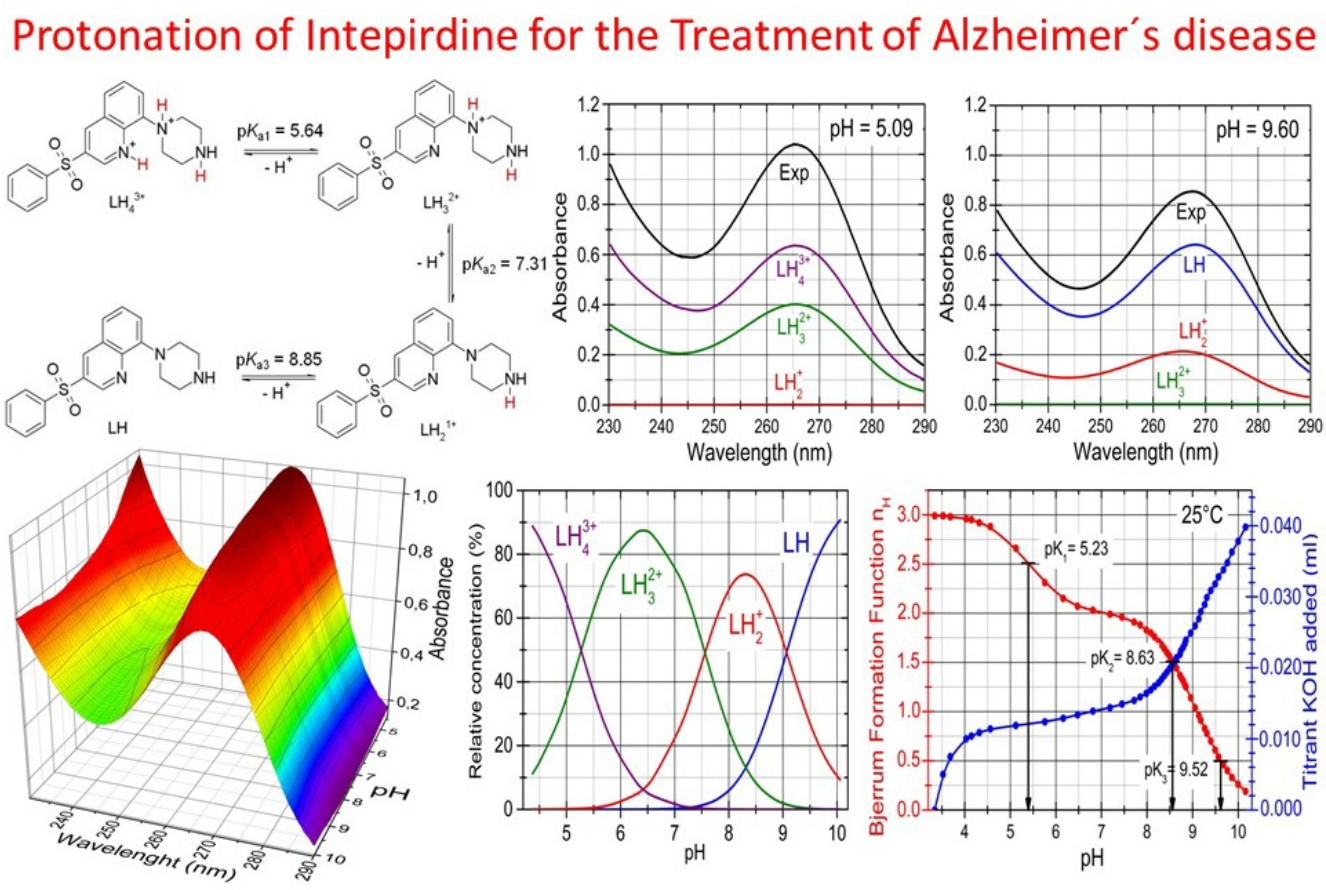

1. INTRODUCTION

Intepirdine (INN) is a novel 5-HT_6 receptor antagonist in development for the treatment of patients with mild-moderate Alzheimer's disease. As a 5-HT_6 receptor antagonist, intepirdine works in part by relieving interneuron-mediated inhibition and promoting the release of acetylcholine and other neurotransmitters in the brain.

Fig. 1

Intepirdine hydrochloride (INN.HCl, developmental codes SB-742457, CAS [607742-55-2] and synonyms RVT-101 GSK 742457 HCl, Intepirdine hydrochloride), is of IUPAC name 3-Phenylsulfonyl-8-(piperazin-1-yl)-quinolone hydrochloride or 3-(Benzenesulfonyl)-8-(piperazin-1-yl)quinoline, $C_{19}H_{19}N_3O_2S.HCl$. MW is 389.90 g/mol. Originaly developed by GSK under the name SB-742457.HCl, RVT-101/Intepirdine hydrochloride HCl is an antagonist of the serotonin receptor 5-HT_6, a largely CNS-specific member of the serotonin receptor subfamily [1]. Intepirdine has also has been reported to reverse both experimentally induced and age-related learning deficits in rats [2] [3]. In December 2014, Axovant Sciences acquired the rights to this drug and renamed it RVT-101 [4-6]. At AAIC 2015, it was presented [7] a more thorough analysis of prior Phase 2b GSK data that had been analyzed previously based on the intent-to-treat population, and came up with a slightly larger effect size on essentially similar efficacy results.

One of the most important physico-chemical characteristics of the drug is considered its pK_a value, which is one of the most prominent parameters applied in pharmacokinetic and bioavailability studies [8-11]. The extent

of the ionization of a compound plays a crucial role in the characterization of its absorption, distribution, metabolism and excretion (ADME) profile. In the case of poorly water soluble drugs the significance of pK_a intensively increases, particularly within the context of its ADME properties [12,13]. The level of general interest in such ionization phenomena is evident from the large number of recent publications on the topic [14-16]**.** pK_a values can be either experimentally measured or theoretically predicted:

1. Many new drugs are poorly soluble in aqueous solutions and conventional potentiometric determination of dissociation constants of these compounds can often be difficult. Spectrophotometry, and UV-titration (also called WApH technique [17]) in particular, is a highly sensitive convenient method to determine pK_a in very diluted aqueous solutions since it requires relatively simple equipment and can work with sub-micromolar compound concentration (about 10^{-5} to 10^{-6} M). The compound should possess pH-dependent distinct spectral responses due to the presence of a chromophore in proximity to the ionization centre *cf. ref.* [18-20]. Zevatskiy [21] describes Standard Spectrophotometric Method (SSM) for obtaining pK_a. This classical method is based on measuring the UV-VIS absorption spectra of prototropic form mixtures at several pH values in the vicinity of the assumed pK_a. The principal limitations of SSM are responsible in UV-titration:

(a) Sufficient resolution of absorption spectra of protonated and deprotonated forms.

(b) The absorbance spectra *vs.* pH must be informative, *i.e.,* it must have at least one maximum of the first or second derivative by pH in the pH area corresponding to the pK_a value.

(c) Preparation of a series of solutions with the constant concentration of analyte and ionic strength in the entire pH range is very time-consuming. The spectrophotometric titration technique is therefore recommended. The authors [22-25] have shown that spectrophotometric titration in combination with suitable chemometric tools can be used to determine dissociation constants pK_a even for sparingly soluble drugs. The most relevant algorithms are SQUAD84 [19] and REACTLAB [26].

2. Nine commercially available or free programs for predicting ionization constants were compared [27]. Meloun et al. [28] used the REGDIA regression diagnostics algorithm written in S-Plus [29] to critically examine the accuracy of pK_a predictions with two programs (ACD/Percepta [30-34,27,35], MARVIN [32,33,36,37,27,38,30,39]) considered the best. Balogh et al. [32] also found the most predictive and reliable predictors to be MARVIN and ACD/Percepta.

The aim of our study was to examine the spectrophotometric analysis of the pH-absorbance matrix with small changes in spectra and to carry out a potentiometric determination of the protonation model to find suitable conditions for a reliable regression determination of dissociation constants.

2. COMPUTATIONAL DETAILS

2.1 UV-metric spectra analysis

Spectrophotometric titration data were treated using the program SQUAD84 [19] and REACTLAB [26] which calculates equilibrium (protonation or dissociation) constants and molar absorptivities of the pure species by nonlinear regression of pH-spectra. The program requires a previous model of the protonation equilibria, based upon the existence of certain chemical species, to be postulated in advanced. The refinement of equilibrium constants is carried out using the nonlinear least-squares algorithm by numerical differentiation, until a minimum

in the Residuals Sum of the Squares (RSS) is attained. The minimization process is repeated until the relative change of RSS between two iterations is less than 0.01 %. The general procedure of the spectrophotometric study of the protonation equilibria called the UV-metric spectra analysis (WApH-technique [17]) has been described [24,25] with the following brief scheme to be shortly submitted here:

Step 1: *Theoretically predicted pK_a estimates:* Two prediction programs, MARVIN and ACD/Percepta provide a set of powerful tools for theoretical predicting pK_a on the structural formulae of the compound.

Step 2: *Instrumental error of absorbance measurement, $s_{inst}(A)$, and the number of light-absorbing species n_c:* The INDICES programme [40] estimates the minimum numbers of light-absorbing species n_c using the Wernimont-Kankare method of factor analysis [40,20] and the instrumental error of absorbance measurement $s_{inst}(A)$. Details may be found on page 104 in ref. [41].

Step 3: *Diagnostics for a search of the chemical model building and testing:* Two regression programs for the numerical analysis of spectra were used, the hard modelling technique SQUAD84 [19] and the soft-modelling technique REACTLAB [28,25,26]. Diagnostic criteria in regression serve to indicate a chemical (protonation) model building and testing. The graphical and numerical analysis of residuals is described in [25,24,22] and a detailed procedure can be briefly stated:

3.1 The physical meaning of parametric estimates: The physical meaning of the dissociation constants and associated molar absorptivities is examined: p$K_{a,i}$ and ε_i should be pursuant neither too high nor too low, and ε_i should not be negative.

3.2 The physical meaning of the species concentrations: Physical constraints are generally applied to concentrations of species and their molar absorptivities as they must be positive numbers. The free concentrations of the basic components and the variously protonated species of the chemical model should show realistic molarities, *i.e.* higher than about 10^{-8} M.

3.3 Goodness-of-fit test using the statistical analysis of residuals: To identify the "best" or true chemical model when several are possible or proposed, to establish whether the chemical model represents the data adequately, the residuals vector ***e*** should be carefully analysed. One of the most important statistics calculated is *the standard deviation of the absorbance*, $s(A)$, estimated at the termination of the regression process as $s(A) = \sqrt{U_{\min}/df}$ where $U_{\min}$ stands for the residuals-square-sum function RSS in minimum and *df* is the degree of freedom, *cf.* page 101 in [41] and page 290 in [42].

3.4 Reproducibility and selection of the spectral range: To examine the dependence of proximity between the ionisable group and the chromophore, the absorbance shift with a change of pH in the efficient wavelengths range may be significant enough to allow for a successful determination.

3.5 The signal-to-error ratio in the analysis of small spectra changes [25]: The absorbance shift Δ_{ij} is the absorbance difference for the *j*th-wavelength at the *i*th-spectrum $\Delta_{ij} = A_{ij} - A_{i,\text{acid}}$, where $A_{i,\text{acid}}$ is the limiting spectrum of the acid form of the drug measured and this Δ_{ij} is then divided by the instrumental standard deviation $s_{inst}(A)$. The resulting ratio $\Delta/s_{inst}(A)$ is called *the signal-to-error ratio SER* and is examined for all absorbance

matrix elements in the whole range of wavelength λ. When the ratio $\Delta/s_{\text{inst}}(A)$ is equal to or higher than 10, the factor analysis is able to predict the correct number of components in the equilibrium mixture.

3.6 The deconvolution of spectra: The resolution of each experimental spectrum into the spectra for the individual variously protonated species shows whether the experimental design, *i.e.* the proposed pH range was efficient enough.

Step 4: *Determination of the thermodynamic dissociation constants* pK_a^T: The limited form of the Debye–Hűckel equation to the data for aqueous solutions, namely for low values of an ionic strength, was applied so that the mixed dissociation constant pK_a is a dependent variable while the ionic strength I is the independent variable. One unknown parameter pK_a^T is estimated by minimizing the sum of squared residuals in the regression analysis.

2.2 pH-metric titration analysis

Potentiometric determination using the ESAB program [43,44] was previously described:

Step 1: *Dissociation constants and mass balance equations:* For dissociation reactions realized at constant ionic strength the so-called "mixed dissociation constants" are defined as $K_{a,j} = \left[H_{j-1}L\right] a_{H^+} / \left[H_jL\right]$. The mass balance equations are $L = l + \sum_{j=1}^{J} \beta_{H_j} l h^j$ and $H = h - \frac{K_w}{h} + j\sum_{j=1}^{J} \beta_{H_j} l h^j$.

Step 2: *Potentiometric readings in pH-titration*: It is obtained with a proton-sensitive glass, and a reference electrodes cell can be described by the equation

$$E_{cell} = E^0 + \frac{f.RT\ln 10}{F}\log a_{H^+} + j_a a_{H^+} - \frac{j_b K_W}{a_{H^+}} - E_{ref} = E^{0'} + S\log h\,.$$

where E^o is the standard potential of a glass electrode cell containing some other constants of the glass electrode as the asymmetry potential, etc., and $a_{H^+} = \left[\mathrm{H}^+\right] y_{H^+} = h y_{H^+}$, a liquid-junction potential E_j is expressed by the term $E_j = j_a a_{H^+} - j_b K_w / a_{H^+}$, and $S = (f.\ RT\ \ln 10)/F$ is the slope of glass electrode for a Nernstian response, K_w is the operational ion product of water at temperature T [K], the correction factor f, is taken as an adjustable parameter. Under a constant ionic strength the activity coefficient does not change, and the term $E^{0'}$ in the *pH* range from 3 to 11 is practically constant.

Step 3: *An explicit equation for the titration curve*: Under constant ionic strength, dependence is expressed between the volume of *titrant* added from burette V_i and the monitored *emf* $E_{cell,i}$ or $pa_{\mathrm{H+}}$ with the vector of unknown parameters (***b***) being separated into the vector of *common parameters* ($\mathbf{K_a}$) and the vector of *group parameters* (**p**), *i. e.* $V_i = f(E_{cell,i}; \mathbf{b}) = f(E_{cell,i}; \mathbf{K_a}, \mathbf{p})$. The vector of common parameters $\mathbf{K_a}$ = $(K_{a,1}, ..., K_{a,m})$ contains m dissociation constants of the acid LH_j. The vector of group parameters **p** = $(E^{0'}, S, K_w, j_a, j_b, L_0, L_T, H_0, H_T)$ contains two constants of the Nernstian equation, $E^{0'}$ and S, and also the total ligand concentration, L_0, and

the hydrogen ion concentration, H_0 of titrand in vessel, and the corresponding quantities of titrant, L_T and H_T in burette. Group parameters $\boldsymbol{p}$ can be refined simultaneously with the common parameters $\boldsymbol{K_a}$.

Step 4: *The regression analysis:* The program ESAB [43,44] is based on a minimization of the sum of squared residuals. It uses the strategy for treating *emf* or pa_{H+} data or the volume of *added titrant V* from burette to find dissociation constants that give the "best" fit to experimental data. As primary data contains the total concentration H_T of proton from burette and the measured pa_{H+}, one could trust pa_{H+} and minimize the residual sum of squares $(V_{exp} - V_{calc})^2$. The residual e is formulated with the volume of *added titrant V* from burette so that $e_i = (V_{exp,i} - V_{calc,i})$ and the resulting residual sum of squares $U(\boldsymbol{b})$ is defined

$$U(\mathbf{b}) = \sum_{i=1}^{n} w_i (V_{\exp,i} - V_{calc,i})^2 = \sum_{i=1}^{n} w_i e_i^2 ,$$

where w_i is the statistical weight usually set equal to unity while in ESAB it may be equal to $\frac{1}{w_i} = s_i^2 = s_E^2 + \left[\frac{dE_i}{dV_i}\right]^2 s_V^2$, and with good equipment we generally have s_E = 0.1 mV or 0.01 pH units and s_V = 0.0005 - 0.0010 cm^3.

3. MATERIALS AND METHODS

3.1 Materials

Intepirdine hydrochloride donated by ZENTIVA k. s., (Prague) with declared purity checked by a HPLC method and alkalimetrically, was always >99%. This drug was weighted straight to a reaction vessel resulting in a concentration of about 9.1×10^{-5} mol. dm^{-3}. Other chemicals were previously described [23].

3.2 Apparatus

The apparatus used and both titration procedures were described in detail [25,28,24]. The experimental and computation scheme to determine the dissociation constants of the multi-component system is taken from Meloun *et al, cf.* page 226 in *ref.* [41] and the all steps are described in details [24]. The free hydrogen-ion concentration $[H^+]$ was measured on the digital voltmeter Hanna HI 3220 with a precision of ±0.002 pH using the combined glass electrode Theta HC 103-VFR. The potentiometric titrations of drugs with potassium hydroxide were performed using a hydrogen activity scale. Standardization of the pH meter was performed using WTW standard buffers values, 4.006 (4.024), 6.865 (6.841) and 9.180 (9.088) at 25°C and 37 °C, respectively, in brackets.

3.3 Software

Estimation of dissociation constants was performed by the nonlinear regression analysis of the UV-metric spectra analysis (WApH-technique) using SQUAD84 [19], REACTLAB [26] programs and potentiometric pH-metric titration data using the ESAB program [43,44], and the spectra interpretation using the INDICES program [40]. Most graphs were plotted using ORIGIN (Ver. 9.1) [45]. ACD/Percepta [30-34,27,35] and MARVIN [32,33,36,37,27,38,30,39]) programs for predictions of pK_a´s are based on the structural formulae of drug

compounds. By entering the compound topological structure descriptors graphically, pK_a values of organic compounds were predicted using approximately hundreds of Hammett and Taft equations and quantum chemistry calculus.

4. RESULTS AND DISCUSSION

The spectrophotometric analysis of the pH-absorbance matrix and the potentiometric determination of the protonation model found suitable conditions for a reliable regression determination of dissociation constants.

4.1 UV-metric A-pH spectra analysis (WApH-technique)

The strategy for efficient experimentation in dissociation constants determination followed by spectral data treatment was used according to our published Tutorial [24]. A qualitative interpretation of the spectra aims to evaluate the quality of the data set, remove spurious data, and estimate the minimum number of factors that contribute aqueous species, which are necessary to describe the experimental data.

Fig. 2

Step 1: *Theoretically predicted pK_a estimates:* MARVIN predicts three ionization sites A, B and C in Fig. 2 that can be associated with dissociation constants; all ionization sites are associated with the nitrogen atom. The macrodissociation constants of Intepirdine (free base) INN were predicted according to the chemical structure analyzed by two reliable pK_a prediction tools. MARVINM pK_a-prediction is based on the calculated partial charge of the atoms located in the analyzed structure, using the Hammett-Taft approach and ACD/Percepta was run using the GALAS model. An inspection of the Intepirdine INN chemical structure reveals three basic centers localized on the nitrogen atoms designed by the letters A, B and C. The electronic nature of all nitrogen atoms differs considerably and all of them are affected by different electronic and steric effects. Hence, in order to facilitate prediction of the particular protonation/dissociation sites, the whole molecule was further subdivided into five auxiliary Fragments 1-5. These representative molecules can be considered as gradually simplified parts of the INN including the particular centers A to C. The predicted pK_a values were compared with the values found for the INN. In protonation center A, the predicted pK_a value of the studied Intepirdine molecule approaches the predicted value of the pK_a helper fragment. Centers B and C occur at the site of the molecule, which forms a more complex conformation. The fragments containing these centers are not affected by the electron field of the rest of the molecule, and therefore their predicted pK_a values differ from pK_a values predicted for the whole molecule [46]. Intepirdine hydrochloride is supposed to behave mostly as a neutral molecule LH in pH 9. When this substance is acidified from pH 9 to 7, the cation LH_2^+ is formed. In changing the pH from 7 to 4, the cation LH_3^{2+} and LH_4^{3+} appeared [47].

Fig. 3

Step 2: *Instrumental error of absorbance measurement, $s_{inst}(A)$, and the number of light-absorbing species n_c:* Intepirdine hydrochloride contains a complicated molecular structure introduced in Fig. 1 and 2 and several protonation equilibria can be monitored spectrophotometrically. The spectral data set in the form of absorbance-response-matrix **A** obtained at various pH values was subjected to factor analysis to determine the number of independent light absorbing species, n_c, using the absorbance matrix rank in the INDICES algorithm [40]. The INDICES indicate the position of break points on the $s_k(A) = f(k)$ curve in the Cattell´s scree plot $s_k(A) = f(k)$ using

the most reliable approaches by Wernimont-Kankare´s $s(A)$, *cf. ref.* [40,20]) and give $k^* = 4$ with the corresponding co-ordinate $s_3(A) = 0.95$ mAU (Fig. 3a). This value also represents the actual instrumental error $s_{inst}(A) = 0.95$ mAU of the experimental equipment with the spectrophotometer CINTRA 5 (GBC, Australia). The number of light-absorbing species n_c helps to establish a protonation model. This means that three dissociation constants will be preferred and four species LH_4^{3+}, LH_3^{2+}, LH_2^{+} and LH are supposed to be present. This latter graph can also be plotted on a logarithmic scale and the number of light-absorbing species n_c can be predicted by finding the point $n_c = k^*$ where the slope of index function $PC(k) = f(k)$ changes, $n_c = 4$, (Fig 3b).

Fig. 4

Step 3: *Diagnostics for a search of the chemical model building and testing:* The hard modeling technique SQUAD84 and soft-modeling technique REACTLAB were used. In both programs the same computational strategy was applied, *i. e.,* the *regression triplet* (criticism of data, model and method), *cf.* ref. [22,42]. The search for the best hypothesis of the chemical (protonation) model containing either one, two or three dissociation constants is shown in Fig. 4. The best regression model was sought by testing three working hypotheses of the protonation model: the first concerning one dissociation constant and the others with two and three dissociation constants. The criterion of reliability between the proposed hypotheses was the goodness-of-fit test applying the criterion $s(A)$. At the same time the estimates of the dissociation constants using two regression programs, *i.e.* SQUAD84 and REACTLAB were also compared, (Table 1). The mean residual $E|e|$ [mAU], the standard deviation of residuals $s(e)$ [mAU] and the Hamilton *R-factor* of relative fitness [%] in SQUAD84 generally showed that better fit of the calculated spectra was always achieved for the protonation model with three dissociation constants. REACTLAB seemed to offer the more reliable parameter estimates as it always reached a better curve fitting than the older program of SQUAD84.

The reliability of the regression parameter estimates may be tested using the following general diagnostics (Fig. 4) as was elucidated in detail in ref [24]:

3.1 *The physical meaning of parametric estimates.* The first diagnostic value indicates whether all of the parametric estimates $pK_{a,i}$ and $\square_i$ have physical meaning and reach realistic values. As the standard deviations $s(pK_{a,i})$ of parameters $pK_{a,i}$ and $s(\square_i)$ of parameters $\square_i$ are significantly smaller than their corresponding parameter estimates, all the variously protonated species are statistically significant at a significance level of $\alpha = 0.05$. In the left part of Fig. 4 there are shown the estimated molar absorptivities of all of the variously protonated species $\square_{LH}$, $\square_{LH2}$, $\square_{LH3}$ and $\square_{LH4}$ of Intepirdine hydrochloride with regard to wavelength. The curves of $\square_{LH3}$ and $\square_{LH4}$ seemed to be close and nearly the same.

3.2 *The physical meaning of the species concentrations.* The second diagnostic examines whether all of the calculated free concentrations of variously protonated species on the distribution diagram of the relative concentration expressed as a percentage have physical meaning, which proved to be the case (right panel of Fig. 4). The distribution diagram shows the protonation equilibria of LH_4^{3+}, LH_3^{2+}, LH_2^{+} and LH. At pH 8 Intepirdine hydrochloride has the species LH and LH_2^{+}. Acidification of the species LH_2^{+} first creates the cation LH_3^{2+}, and in a solution of pH 4 to pH 5 predominate cations LH_3^{2+} and LH_4^{3+}. At concentrations of 10^{-4} to 10^{-6} M the Intepirdine hydrochloride is sufficiently soluble and all its dissociation constants can therefore be spectrophotometrically determined.

3.3 *Goodness-of-fit test:* Although the statistical analysis of residuals [24] gives the most rigorous test of the goodness-of-fit, realistic empirical limits must be used. The statistical measures of all residuals *e* prove that the minimum of the elliptic hyperparaboloid *RSS* has been reached (Table 1): the mean residual $E\left|\bar{e}\right|$ [mAU] and the standard deviation of residuals $s(\hat{e})$ [mAU] always have sufficiently low values, lower than 2 mAU, which is less than 0.2% of the measured absorbance value proving so a good fitness. This is also proven by small value of the Hamilton *R-factor.*

Fig. 5

3.4 *Reproducibility and a selection of the spectral range:* To examine the dependence of the proximity between the ionisable group and the chromophore, the spectral shift may not be strong enough to allow for a successful determination. The absorbance data were first subjected to factor analysis to evaluate the number of light-absorbing species in Fig. 3 and Table 1. The spectra set of useful analytical wavelengths ranges 230 – 290 nm was examined to indicate the best wavelength range 230 – 260 nm and 250 – 290 nm in which the actual chromophore is active and reflects the protonation equilibria model in the molecule (Fig 5). Three dissociation constants pK_{a1}, pK_{a2}, pK_{a3}, and four molar absorptivities of Intepirdine hydrochloride ε_{LH}, ε_{LH2}, ε_{LH3} and ε_{LH4} were estimated using SQUAD84 and REACTLAB in the first run. To check a reproducibility the dissociation constants treated with SQUAD84 and REACTLAB estimated from six reproduced measurements were found to be in good agreement (Table 1). The SQUAD84 approach has a great advantage in a rigorous goodness-of-fit test made by the advanced statistical analysis of residuals. Reproducibility of six experimental spectra sets in 230 – 290 nm shows that three dissociation constants lead to mean values pK_{a1} 5.53, pK_{a3} 7.58 and pK_{a4} 8.93 with $s(A)$ = 1.41 mAU are well-conditioned in the regression model, and therefore their numerical evaluation is quite reliable here.

Fig. 6

3.5 *Signal-to-error ratio in analysis of small spectra changes*: In the spectrophotometric determination of pK_a of the Intepirdine hydrochloride it is necessary to investigate whether the change in pH will cause a sufficient change in absorbance in shape of a spectrum. Fig. 6a shows that the spectral response on the chromophore in the INN.HCl molecule is not large, so it was necessary to test whether it is possible to estimate the dissociation constants even from such small spectrum changes. Fig. 6b shows the A-pH curve at selected wavelengths of the UV spectrum, depending on the pH, which demonstrates changes in the absorbance at pH change. Plot of small absorbance changes in the Intepirdine spectrum within pH-titration when the value of the absorbance difference for the *j*th-wavelength of the *i*th-spectrum $SER_{ij} = A_{ij} - A_{i,acid}$ is calculated and then divided with the instrumental standard deviation, leading to $SER/s_{inst}(A)$. The resulting ratio of the normalized spectra changes $SER = \Delta/s_{inst}(A)$ is plotted versus the wavelength λ for all absorbance matrix elements (Fig. 6c). The *SER* ratio is then compared to the limiting *SER* value to test if the small absorbance changes are still significantly larger than the instrumental noise. It is known from past experience that when the *SER* value is greater than 10, a factor analysis will be able to predict the correct number of light-absorbing components in the equilibrium mixture. To prove that the non-linear regression can analyze such spectral data, the residuals set was compared to the instrumental noise, $s_{inst}(A)$. Fig. 6d shows a comparison of the ratio of the residuals of spectra normalized against

instrumental noise, $e/s_{inst}(A)$, and plotted versus the wavelength. It is clear that most of the residuals are of nearly the same magnitude as the instrumental noise and that the ratio $e/s_{inst}(A)$ is less than ±2.

Fig. 7

3.6 *The deconvolution of spectra.* Fig. 7 presents six figures of experimental spectra deconvolution from pH 5.09 through 9.60 to show the consecutive deprotonation response in spectra, when each experimental spectrum was decomposed into the spectra of differently protonated species in of Intepirdine hydrochloride mixture. At pH 5.09 the cation LH_4^{3+} accompanying cation LH_3^{2+} predominates in the solution. At pH 5.52 together with the cation LH_3^{2+} one dominant species LH_4^{3+} exhibits an absorption band at the same wavelength of the absorption maximum λ_{max}. At pH 7.21 and 8.14 the experimental spectrum is decomposed into two absorption bands concerning the cation LH_3^{2+} and LH_2^{+}. At pH = 8.86 the neutral molecule LH occurs with cation LH_2^{+}, and the concentration of LH in the solution increases up to pH 9.60.

Step 4: *Determination of the thermodynamic dissociation constants:* An examination of the effect of ionic strength on the protonation of chromophore in Intepirdine hydrochloride is obvious from the dependence of the spectra shape on the ionic strength, at a low value of ionic strength, the λ_{max} of the chromophore corresponding to the individual species LH_4^{3+}, LH_3^{2+}, LH_2^{+} and LH is not significantly affected. The mixed dissociation constant determined at various values of ionic strength were extrapolated according to the limited Debye-Hückel law to the zero value of ionic strength and thermodynamic values were obtained at two temperatures 25℃ and 37℃ (Fig. 9).

Table 1

4.2 pH-metric data analysis

The potentiometric titration of a mixture of HCl and Intepirdine hydrochloride with potassium hydroxide concerning the pH-metric data analysis was carried out at 25℃ and 37℃ for the adjusted value of ionic strength (Fig. 8). The initial tentative value of the dissociation constant of the Intepirdine hydrochloride studied, corresponding to the midpoint value in each plateau of the potentiometric titration curve, was refined by the ESAB program.

Fig. 8

Since Intepirdine hydrochloride exhibits three dissociation constants, their numerical estimation is performed using computer-assisted nonlinear regression. Regression analysis was employed by using a plateau of the middle part titration curve which concerned alkalized Intepirdine hydrochloride titrated with hydrochloric acid, followed by a subsequent retitration with potassium hydroxide. Also calculated on the assessed point titration curve was the Bjerrum formation protonation function, which is shown in the graph in Fig. 8. The estimates of the three dissociation constants pK_{a1}, pK_{a2}, and pK_{a3} are plotted on the Bjerrum formation curves. Since pH above 10 and pH below 4 in a titrated solution a very fine precipitate of Intepirdine hydrochloride occurs that initially forms a slight opalescence. This part of the titration curve with pH over 10 and pH below 4 did not undergo regression analysis only for estimating pK_{a1}, pK_{a2}, and pK_{a3}.

Table 2

The ESAB residuals are defined as the difference between the experimental and calculated titrant volume. The goodness-of-fit test is performed with the statistical analysis of residuals. As further group parameters are refined, the fit is improved. A quite sensitive criterion of the reliability of the dissociation constants estimated is the mean of absolute values of residuals $E\,|\,\bar{e}\,|$ [mL]. Comparing residuals with the instrumental noise, $s_{\mathrm{inst}}(V)$, represented here by either $s_{\mathrm{inst}}(V) = s(V) = 0.0001$ mL, an excellent fit is confirmed since the mean $E\,|\,\bar{e}\,|$ [mL] and also the residual standard deviation $s(\hat{e})$ [mL] are nearly the same, and are lower than the experimental noise $s_{inst}(y)$. Here, $E\,|\,\bar{e}\,| = 0.0001$ mL and $s(\hat{e}) = 0.0001$ mL are similar and both are the same as the microburette error $s(V) = 0.0001$ mL. All residuals oscillate between the lower -0.0001 mL and upper limit 0.0001 mL of Hoaglin´s inner bounds and therefore no outlying residuals were indicated outside these bounds (*cf.* page 80 in ref. [48]). The estimates of the dissociation constants estimated by ESAB are reliable (Table 2). The curve-fittness is significantly improved using the refinement of the group parameter L_0, the concentration of the titrated drug Intepirdine hydrochloride.

Fig. 9

Fig. 9 brings the extrapolation of the mixed dissociation constants to the zero value of ionic strength according to the limited Debye-Hückel law for the protonation model of two and three dissociation constants at temperatures 25^0C and 37^0C.

4.3 Comparison of the experimental pK_a values with the literature data

Spectroscopic titration has been utilized as an alternative to determine pK_a values of substances with large molar absorptivities because of its high sensitivity to concentrations of substance as low as 10^{-5} M. However, the examined compound must posses chromophore(s) in proximity to the ionization center(s) so that the protonated and deprotonated species exhibit sufficient spectral dissimilarity. In UV titration, the spectral data of Intepirdine hydrochloride measured are a series of spectra acquired at different pH values. Acidifying the solution of the species LH_2^+ leading to cations LH_3^{2+} and LH_4^{3+} may be disturbed by Intepirdine hydrochloride precipitation which manifests itself especially at higher concentrations in potentiometric determination. Both REACTLAB and SQUAD84 programs for spectra analysis produce for the spectrophotometric concentration 9.2×10^{-5} M Intepirdine hydrochloride the same estimates of all three dissociation constants which exhibit identical goodness-of-fit test. The influence of temperature at 25℃ and 37℃ does not seem to be too significant.

The ESAB program minimizing residuals $e_i = (V_{exp,\,i} - V_{calc,\,i})$ reaches 0.1 or 0.2 microlitres, thus proving an excellent fit. It may be concluded that the reliability of the dissociation constants of Intepirdine hydrochloride was proven though the *group parameters* L_0, H_T were ill-conditioned in the model. The goodness-of-fit proved sufficient reliability of the parameter estimates for three dissociation constants of the Intepirdine hydrochloride at 25°C and 37°C. The determined dissociation constants are in agreement with the predicted values from the MARVIN program as stated in the results. The discrepancy might be caused by the unclear resonance structure of the heterocyclic core, and, consequently, different electron distribution, which can further lead to different predicted values according to the proposed structure. Moreover, there is a mutual, both electronic and spatial, interaction between the centers A and B, which further complicates estimation of their pK_a values. In such cases,

the prediction programs MARVIN and ACD/Percepta may fail, and experimental laboratory determination is needed. As both potentiometric and spectrophotometric results are similar regarding the goodness-of-fit tests, the conclusion can be drawn that the obtained experimental results are reliable and that they show the real dissociation of the substance.

Scheme 1

As shown in Fig. 2, the INN possesses three nitrogen basic centers, which may undergo protonation/dissociation. Quinoline can be considered as the fundamental π-conjugated scaffold of the INN. Whereas the conjugated acid of unsubstituted quinoline possesses pK_a 4.94, the pK_a values of aminoquinolines range from 3.99 to 9.17 (in water) as a function of the amino group positioning [47]. For instance, 7-aminoquinoline possesses pK_a 6.65 whereas shifting the amino group to the position 8 (as in the INN) dramatically decreases the pK_a to 3.99. This is mostly caused by hydrogen bonding between two neighbor basic sites A and B (Fig. 2). We can suppose that phenylsulphonyl group attached at the non-conjugating position 3 has only little electronic effect on the centers A and B. The diminished effect can be for example demonstrated by comparing pK_a values of 3-aminoquinoline (4.95) and unsubstituted quinoline (4.94), which are almost identical [47]. On the other hand, a direct donor-acceptor interaction between *N*,*N*-dialkylamino group (center B) and quinoline (center A) increases basicity of the center A and, simultaneously, improves the acidity of the center B. For instance, a conjugated acid of *N*,*N*-diethylaniline (Fragment 4) has pK_a 6.57 [48], whereas the measured values is 5.51. The center C localized on the piperazine ring can be considered as a *N*,*N*-dialkylamine and, therefore, possesses the highest basicity with the highest measured pK_a of the corresponding conjugated acid (8.93). For instance, *N*,*N*-diethylamine (Fragment 5) possesses pK_a of 10.84 [48]. Based on this comparison, we can assign the three observed dissociation constants pK_{a1}, pK_{a2} and pK_{a3} to deprotonation of the particular centers A, B and C (Scheme 1).

5. CONCLUSION

Spectrophotometric and potentiometric pH-titration allowed the measurement of three dissociation constants of Intepirdine hydrochloride (Scheme 1), but worse solubility at pH above 10 and also pH below 4 for the Intepirdine hydrochloride concentration of micromoles leads to the conclusion that an estimation of pK_a higher than 10 and in potentiometry lower than 4 is not reliable enough.

1) The sparingly soluble neutral molecule LH of Intepirdine hydrochloride capable of protonation to form the still soluble three cations LH_2^+, LH_3^{2+} and LH_4^{3+} occurs in pure water. The graph of molar absorption coefficients of variously protonated species according to wavelength shows that the spectrum of species LH_2^+ and LH vary in colour, while protonation of chromophore LH_2^+ to LH_3^{2+} and LH_4^{3+} has less influence on chromophores in Intepirdine hydrochloride molecule.

2) We have proven that in the range of pH 4 to 10 three dissociation constants can be reliably estimated from the spectra when concentration of Intepirdine hydrochloride is about 9.2×10^{-5} mol.dm^{-3}. Although the somewhat less

affected pH changes in the chromophore, three thermodynamic dissociation constants can be reliably determined with SQUAD84 and REACTLAB reaching the similar values with both programs, pK^{T}_{a1} = 5.64, pK^{T}_{a2} = 7.31, pK^{T}_{a3} = 8.85 at 25°C and pK^{T}_{a1} = 5.51, pK^{T}_{a2} = 7.15, pK^{T}_{a3} = 8.77 at 37°C.

3) Three thermodynamic dissociation constants of Intepirdine hydrochloride in a potentiometric concentration of 3×10^{-4} mol.dm^{-3} were determined by the regression analysis of potentiometric titration curves using ESAB, pK^{T}_{a1} = 5.14, pK^{T}_{a2} = 8.38, pK^{T}_{a3} = 9.33 at 25°C and pK^{T}_{a1} = 5.17, pK^{T}_{a2} = 8.31, pK^{T}_{a3} = 9.07 at 37°C.

4) Prediction of the dissociation constants of Intepirdine hydrochloride was performed using the MARVIN program to specify protonation locations and using the ACD/Percepta program. In comparising two predictive and two experimental techniques, it may be concluded that the prediction programs often vary in estimating pK_a.

LITERATURE CITED:

1. Upton, N., Chuang, T.T., Hunter, A.J., Virley, D.J.: 5-HT6 receptor antagonists as novel cognitive enhancing agents for Alzheimer's disease. Neurotherapeutics **5**(3), 458-469 (2008)
2. Callaghan, C.K., Hok, V., Della-Chiesa, A., Virley, D.J., Upton, N., O'Mara, S.M.: Age-related declines in delayed non-match-to-sample performance (DNMS) are reversed by the novel 5HT6 receptor antagonist SB742457. Neuropharmacology **63**(5), 890-897 (2012)
3. Codony, X., Vela, J.M., Ramirez, M.J.: 5-HT6 receptor and cognition. Current Opinion in Pharmacology **11**(1), 94-100 (2011)
4. Lombardo, I., Ramaswamy, G., Friedhoff, L., Asare, E.: Intepirdine (RVT-101), a 5-HT6 Receptor Antagonist, as an Adjunct to Donepezil in Mild-to-Moderate Alzheimer's Disease: Efficacy on Activities of Daily Living Domains. Am J Geriat Psychiat **25**(3), S120-S121 (2017)
5. Ferrero, H., Solas, M., Francis, P.T., Ramirez, M.J.: Serotonin 5-HT6 Receptor Antagonists in Alzheimer's Disease: Therapeutic Rationale and Current Development Status. Cns Drugs **31**(1), 19-32 (2017)
6. de Bruin, N.M.W.J., van Loevezijn, A., Wicke, K.M., de Haan, M., Venhorst, J., Lange, J.H.M., de Groote, L., van der Neut, M.A.W., Prickaerts, J., Andriambeloson, E., Foley, A.G., van Drimmelen, M., van der Wetering, M., Kruse, C.G.: The selective 5-HT6 receptor antagonist SLV has putative cognitive- and social interaction enhancing properties in rodent models of cognitive impairment. Neurobiol Learn Mem **133**, 100-117 (2016)
7. Mason, V.L.: Alzheimer's Association International Conference on Alzheimer's Disease 2015 (Aaic 2015) (July 18-23, 2015-Washington, Dc, USA). Drug Today **51**(7), 447-452 (2015)
8. Pathare, B., Tambe, V., Patil, V.: A review on various analytical methods used in determination of dissociation constant. International Journal of Pharmacy and Pharmaceutical Sciences **6**(8), 26-34 (2014)
9. Reijenga, J., Hoof, A.v., Loon, A.v., Teunissen, B.: Development of Methods for the Determination of pKa Values. Anal. Chem. Insights **8**, 53-71 (2013)
10. Hernández, J.A., Hernández, A.R., Urbina, E.M.C., Rodríguez, I.M.D.L.G., Manzanares, M.V., Medina-Vallejo, L.F.: New chemometric strategies in the spectrophotometric determination of pKa. European Journal of Chemistry **5**(1), 1-5 (2014)
11. Shayesteh, T.H., Radmehr, M., Khajavi, F., Mahjub, R.: Application of chemometrics in determination of the acid dissociation constants (pK(a)) of several benzodiazepine derivatives as poorly soluble drugs in the presence of ionic surfactants. Eur J Pharm Sci **69**, 44-50 (2015)
12. Pandey, M.M., Jaipal, A., Kumar, A., Malik, R., Charde, S.Y.: Determination of pK(a) of felodipine using UV-Visible spectroscopy. Spectrochim Acta A **115**, 887-890 (2013)

13. Manallack, D.T.: The pK(a) Distribution of Drugs: Application to Drug Discovery. Perspect Medicin Chem **1**, 25-38 (2007)
14. Milletti, F., Storchi, L., Sforna, G., Cruciani, G.: New and original pKa prediction method using grid molecular interaction fields. J. Chem. Inf. Model. **47**, 2172-2181 (2007)
15. Settimo, L., Bellman, K., Knegtel, R.A.: Comparison of the accuracy of experimental and predicted pKa values of basic and acidic compounds. Pharm. Res. **31**, 1082-1095 (2014)
16. Tam, K.Y., Takacs-Novak, K.: Multiwavelength spectrophotometric determination of acid dissociation constants: A validation study. Anal. Chim. Acta **434**, 157-167 (2001)
17. Allen, R.I., Box, K.J., Comer, J.E.A., Peake, C., Tam, K.Y.: Multiwavelength spectrophotometric determination of acid dissociation constants of ionizable drugs. Journal of Pharmaceutical and Biomedical Analysis **17**(4-5), 699-712 (1998)
18. Hartley, F.R., Burgess, C., Alcock, R.M.: Solution Equilibria. Ellis Horwood, Chichester (1980)
19. Leggett, D.J., McBryde, W.A.E.: General computer program for the computation of stability constants from absorbance data. Analytical Chemistry **47**(7), 1065-1070 (1975)
20. Kankare, J.J.: Computation of equilibrium constants for multicomponent systems from spectrophotometric data. Analytical Chemistry **42**(12), 1322-1326 (1970)
21. Zevatskiy, Y.E., Ruzanov, D.O., Samoylov, D.V.: Photometric method for determination of acidity constants through integral spectra analysis. Spectrochim Acta A **141**, 161-168 (2015)
22. Meloun, M., Ferenčíková, Z., Javůrek, M.: Reliability of dissociation constants and resolution capability of SQUAD(84) and SPECFIT/32 in the regression of multiwavelength spectrophotometric pH-titration data. Spectrochim Acta A Mol Biomol Spectrosc **86**, 305-314 (2012)
23. Meloun, M., Nečasová, V., Javůrek, M., Pekárek, T.: The dissociation constants of the cytostatic bosutinib by nonlinear least-squares regression of multiwavelength spectrophotometric and potentiometric pH-titration data. Journal of Pharmaceutical and Biomedical Analysis **120**, 158-167 (2016)
24. Meloun, M., Bordovská, S., Syrový, T., Vrána, A.: Tutorial on a chemical model building by least-squares non-linear regression of multiwavelength spectrophotometric pH-titration data. Anal Chim Acta **580**(1), 107-121 (2006)
25. Meloun, M., Bordovská, S., Vrána, A.: The thermodynamic dissociation constants of the anticancer drugs camptothecine, 7-ethyl-10-hydroxycamptothecine, 10-hydroxycamptothecine and 7-ethylcamptothecine by the least-squares nonlinear regression of multiwavelength spectrophotometric pH-titration data. Anal Chim Acta **584**(2), 419-432 (2007)
26. Maeder, M., King, P.: Analysis of Chemical Processes, Determination of the Reaction Mechanism and Fitting of Equilibrium and/or Rate Constants. (2012)
27. Liao, C.Z., Nicklaus, M.C.: Comparison of Nine Programs Predicting pK(a) Values of Pharmaceutical Substances. J Chem Inf Model **49**(12), 2801-2812 (2009)
28. Meloun, M., Syrový, T., Bordovská, S., Vrána, A.: Reliability and uncertainty in the estimation of pK (a) by least squares nonlinear regression analysis of multiwavelength spectrophotometric pH titration data. Anal Bioanal Chem **387**(3), 941-955 (2007)
29. StatSci: S-PLUS 8.2 a new philosophy of data analysis. http://www.insightful.com/products/splus (1994). 1994
30. Ribeiro, A.R., Schmidt, T.C.: Determination of acid dissociation constants (pK(a)) of. cephalosporin antibiotics: Computational and experimental approaches. Chemosphere **169**, 524-533 (2017)
31. ACD/Labs pKa Predictor 3.0. In: Inc., A.C.D. (ed.). Toronto, Canada, (2007)
32. Balogh, G.T., Gyarmati, B., Nagy, B., Molnar, L., Keseru, G.M.: Comparative Evaluation of in Silico pK(a) Prediction Tools on the Gold Standard Dataset. Qsar Comb Sci **28**(10), 1148-1155 (2009)
33. Balogh, G.T., Tarcsay, A., Keseru, G.M.: Comparative evaluation of pK(a) prediction tools on a drug discovery dataset. Journal of Pharmaceutical and Biomedical Analysis **67-68**, 63-70 (2012)
34. Evagelou, V., Tsantili-Kakoulidou, A., Koupparis, M.: Determination of the dissociation constants of the cephalosporins cefepime and cefpirome using UV spectrometry and pH potentiometry. Journal of Pharmaceutical and Biomedical Analysis **31**(6), 1119-1128 (2003)

35. Roda, G., Dallanoce, C., Grazioso, G., Liberti, V., De Amici, M.: Determination of Acid Dissociation Constants of Compounds Active at Neuronal Nicotinic Acetylcholine Receptors by Means of Electrophoretic and Potentiometric Techniques. Anal Sci **26**(1), 51-54 (2010)
36. Bezencon, J., Wittwer, M.B., Cutting, B., Smiesko, M., Wagner, B., Kansy, M., Ernst, B.: pK(a) determination by H-1 NMR spectroscopy - An old methodology revisited. Journal of Pharmaceutical and Biomedical Analysis **93**, 147-155 (2014)
37. Hansen, N.T., Kouskoumvekaki, I., Jorgensen, F.S., Brunak, S., Jonsdottir, S.O.: Prediction of pH-dependent aqueous solubility of druglike molecules. J Chem Inf Model **46**(6), 2601-2609 (2006)
38. Manchester, J., Walkup, G., Rivin, O., You, Z.P.: Evaluation of pK(a) Estimation Methods on 211 Drug like Compounds. J Chem Inf Model **50**(4), 565-571 (2010)
39. ten Brink, T., Exner, T.E.: pK(a) based protonation states and microspecies for protein-ligand docking. J Comput Aid Mol Des **24**(11), 935-942 (2010)
40. Meloun, M., Čapek, J., Mikšík, P., Brereton, R.G.: Critical comparison of methods predicting the number of components in spectroscopic data. Anal Chim Acta **423**(1), 51-68 (2000)
41. Meloun, M., Havel, J., Högfeldt, E.: Computation of solution equilibria: A guide to methods in potentiometry, extraction, and spectrophotometry. Ellis Horwood series in analytical chemistry. Ellis Horwood Chichester, England (1988)
42. Meloun, M., Militký, J., Forina, M.: Chemometrics for analytical chemistry, Volume 2: PC- aided regression and related methods. Chemometrics for analytical chemistry. Ellis Horwood, Chichester (1994)
43. Rigano, C., Grasso, M., Sammartano, S.: Computer-Analysis of Equilibrium Data in Solution - a Compact Least-Squares Computer-Program for Acid-Base Titrations. Annali Di Chimica **74**(7-8), 537-532 (1984)
44. De Stefano, C., Princi, P., Rigano, C., Sammartano, S.: Computer analysis of equilibrium data in solution ESAB2M: an improved version of the ESAB program. Annali Di Chimica **77**(7-8), 643-675 (1987)
45. ORIGIN. In. OriginLab Corporation, One Roundhouse Plaza, Suite 303, Northampton, MA 01060, USA.,
46. Albert, A., Goldacre, R., Phillips, J.: The Strength of Heterocyclic Bases. J Chem Soc(Dec), 2240-2249 (1948)
47. Perrin, D.D.: Dissociation constants of organic bases in aqueous solution. Butterworths, London (1965)
48. Meloun, M., Militký, J., Forina, M.: Chemometrics for analytical chemistry, Volume 1: PC-Aided Statistical Data Analysis. Chemometrics for analytical chemistry. Ellis Horwood, Chichester (1992)

Figure captions:

Fig. 1 Structural formula of Intepirdine hydrochloride, INN.HCl.

Fig. 2 Molecular structure of Intepirdine INN (inset) with highlighted basic centres A, B and C and predicted pK_a values using MARVIN/ACD prediction programs. Structure of auxiliary fragments 1-5 and their predicted pK_a.

Fig. 3 Upper: The Cattel's scree plot $s_k(SV) = f(k)$ of the of singular value decomposition SVD for the rank estimation of the absorbance matrix $k^* = 4$ in normal scale for INN.HCl. **Lower:** The Cattel's scree plot $\log(s_k(SV)) = f(k)$ in logarithmic scale which leads to four light-absorbing species in the equilibrium mixture, $n_c = 4$. (INDICES in S-PLUS, ORIGIN 9).

Fig. 4 Typical SQUAD84 working environment searching the best protonation model of Intepirdine hydrochloride, INN.HCl in the pH range from 4 to 10 for one (**Upper**), two (**Middle**) and three (**Lower**) dissociation constants pK_{a1}, pK_{a2}, pK_{a3} using 5.46×10^{-5} M INN.HCl at $I = 0.0081$ at 25°C. **Left column:** The

pure spectra profiles of molar absorptivities *vs*. wavelength (nm) for all of the variously protonated species of INN.HCl. **Right column:** The distribution diagram of the relative concentrations of all of the variously protonated species in dependence on pH, (REACTLAB, ORIGIN 9).

Fig. 5 Left column: The plot of the 3D-absorbance-response-matrix for Intepirdine hydrochloride INN.HCl. **Middle column:** The plot of the 2D-absorbance-response-matrix representing the measured multiwavelength absorption spectra for INN.HCl according to pH at 25°C. INN.HCl in aqueous medium of phosphate buffer with adjusted ionic strength 2 M (KCl) was titrated by HCl to pH 2 and after a subsequent retitration with KOH to pH 11 at 25°C. **Right column:** Reproducibility of the estimated dissociation constants evaluated in three absorption bands: **A. Upper:** The absorption band regards 230 to 290 nm. **B. Middle:** This band regards 230 to 250 nm. **C. Lower:** This band regards 250 to 290 nm. The estimates of dissociation constants pK_{a1}, pK_{a2}, and pK_{a3} with their standard deviation in the last two digits are written. The goodness-of-fit is expressed on the right axis of the plot as the standard deviation of absorbance after the regression was performed $s(A)$ [mAU], (REACTLAB, SQUAD84, ORIGIN 9).

Fig. 6 (a) Plot of small absorbance changes in the Intepirdine hydrochloride 2D-spectra set within pH-titration, (b) Absorbance-pH curves at selected wavelengths, (c) Plot of small absorbance shift in the INN.HCl spectrum within pH-titration when the value of the absorbance difference for the *j*th-wavelength of the *i*th-spectrum $SER_{ij} = A_{ij} - A_{i,\text{acid}}$ is divided with the instrumental standard deviation, leading to $SER/s_{\text{inst}}(A)$. This ratio is plotted on wavelength λ. Here $A_{i,\text{acid}}$ is the limiting spectrum of the acid form of the drug, (d) Residuals ***e*** [mAU] are divided by the instrumental standard deviation $e/s_{\text{inst}}(A)$ to test if the residuals ***e*** are of the same magnitude as the instrumental noise $s_{\text{inst}}(A)$, (REACTLAB, ORIGIN 9).

Fig. 7 Deconvolution of the each experimental spectrum of 5.46×10^{-5} M INN.HCl at $I = 0.0081$ at 25°C into spectra of the individual variously protonated species LH, LH_2^+, LH_3^{2+}, LH_4^{3+} in mixture for pH: 5.09, 5.52, 7.21, 8.14, 8.86, and 9.60 using SQUAD84.

Fig. 8 The search for the protonation model analysing the potentiometric titration curve of acidified INN.HCl plus HCl and titrated with KOH and plotted with the Bjerrum protonation function indicating three pK_a values. Dissociation constants are estimated with ESAB at 25°C (**upper**) and 37°C (**lower**) (ESAB, ORIGIN).

Fig. 9 Dependence of the mixed dissociation constants of INN.HCl on the square root of the ionic strength for three dissociation constants leading to the thermodynamic dissociation constant pK_a^T at 25°C **(left)** and 37°C **(right)** using UV-metric technique (**S, Upper**) and pH-metric (**P, Lower**).

Figure captions:

Fig. 1 Structural formula of Intepirdine hydrochloride, INN.HCl.

Fig. 2 Molecular structure of Intepirdine INN (inset) with highlighted basic centres A, B and C and predicted pK_a values using MARVIN/ACD prediction programs. Structure of auxiliary fragments 1-5 and their predicted pK_a.

Fig. 3 Upper: The Cattel's scree plot $s_k(SV) = f(k)$ of the of singular value decomposition SVD for the rank estimation of the absorbance matrix $k^* = 4$ in normal scale for INN.HCl. **Lower:** The Cattel's scree plot $\log(s_k(SV)) = f(k)$ in logarithmic scale which leads to four light-absorbing species in the equilibrium mixture, $n_c = 4$. (INDICES in S-PLUS, ORIGIN 9).

Fig. 4 Typical SQUAD84 working environment searching the best protonation model of Intepirdine hydrochloride, INN.HCl in the pH range from 4 to 10 for one (**Upper**), two (**Middle**) and three (**Lower**) dissociation constants pK_{a1}, pK_{a2}, pK_{a3} using 5.46×10^{-5} M INN.HCl at $I = 0.0081$ at 25°C. **Left column:** The pure spectra profiles of molar absorptivities *vs*. wavelength (nm) for all of the variously protonated species of INN.HCl. **Right column:** The distribution diagram of the relative concentrations of all of the variously protonated species in dependence on pH, (REACTLAB, ORIGIN 9).

Fig. 5 Left column: The plot of the 3D-absorbance-response-matrix for Intepirdine hydrochloride INN.HCl. **Middle column:** The plot of the 2D-absorbance-response-matrix representing the measured multiwavelength absorption spectra for INN.HCl according to pH at 25°C. INN.HCl in aqueous medium of phosphate buffer with adjusted ionic strength 2 M (KCl) was titrated by HCl to pH 2 and after a subsequent retitration with KOH to pH 11 at 25°C. **Right column:** Reproducibility of the estimated dissociation constants evaluated in three absorption bands: **A. Upper:** The absorption band regards 230 to 290 nm. **B. Middle:** This band regards 230 to 250 nm. **C. Lower:** This band regards 250 to 290 nm. The estimates of dissociation constants pK_{a1}, pK_{a2}, and pK_{a3} with their standard deviation in the last two digits are written. The goodness-of-fit is expressed on the right axis of the plot as the standard deviation of absorbance after the regression was performed $s(A)$ [mAU], (REACTLAB, SQUAD84, ORIGIN 9).

Fig. 6 (a) Plot of small absorbance changes in the Intepirdine 2D-spectra set within pH-titration, **(b)** Absorbance-pH curves at selected wavelengths, **(c)** Plot of small absorbance shift in the INN.HCl spectrum within pH-titration when the value of the absorbance difference for the *j*th-wavelength of the *i*th-spectrum $SER_{ij} = A_{ij} - A_{i,\text{acid}}$ is divided with the instrumental standard deviation, leading to $SER/s_{\text{inst}}(A)$. This ratio is plotted on wavelength λ. Here $A_{i,\text{acid}}$ is the limiting spectrum of the acid form of the drug, **(d)** Residuals ***e*** [mAU] are divided by the instrumental standard deviation $e/s_{\text{inst}}(A)$ to test if the residuals ***e*** are of the same magnitude as the instrumental noise $s_{\text{inst}}(A)$, (REACTLAB, ORIGIN 9).

Fig. 7 Deconvolution of the each experimental spectrum of 5.46×10^{-5}M INN.HCl at $I = 0.0081$ at 25°C into spectra of the individual variously protonated species LH, LH_2^+, LH_3^{2+}, LH_4^{3+} in mixture for pH: 5.09, 5.52, 7.21, 8.14, 8.86, and 9.60 using SQUAD84.

Fig. 8 The search for the protonation model analysing the potentiometric titration curve of acidified INN.HCl plus HCl and titrated with KOH and plotted with the Bjerrum protonation function indicating three pK_a values. Dissociation constants are estimated with ESAB at 25°C (**Upper**) and 37°C (**Lower**) (ESAB, ORIGIN).

Fig. 9 Dependence of the mixed dissociation constants of INN.HCl on the square root of the ionic strength for three dissociation constants leading to the thermodynamic dissociation constant pK_a^T at 25°C **(left)** and 37°C **(right)** using UV-metric technique (**S, Upper**) and pH-metric (**P, Lower**).

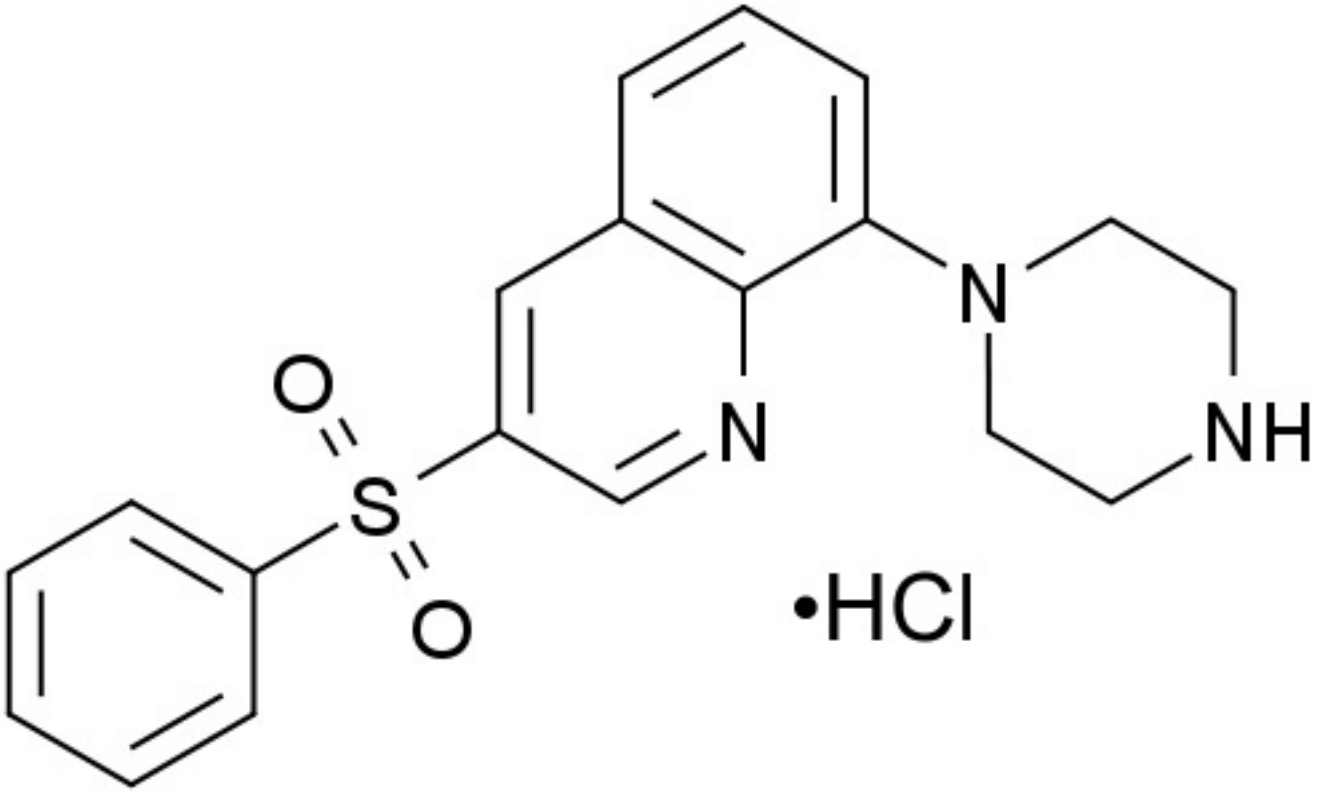
O
S
O
N
N
NH
•HCl

Predicted pK_{pred} of Intepirdine with MARVIN and ACD

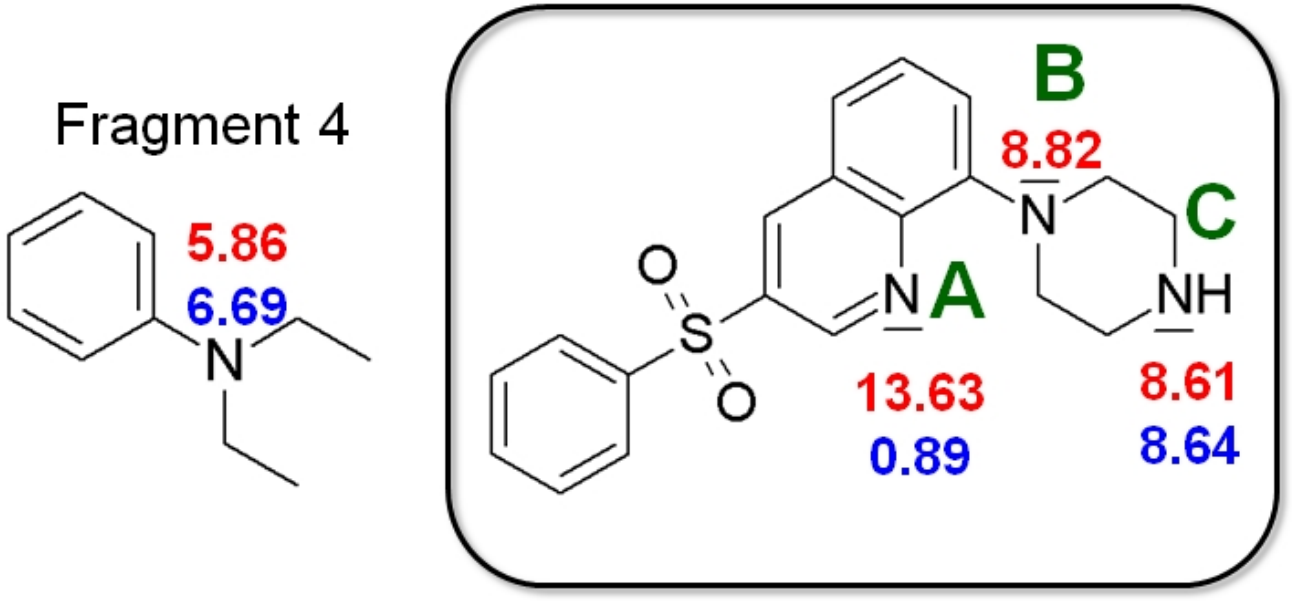

Fragment 4

Fragment 5

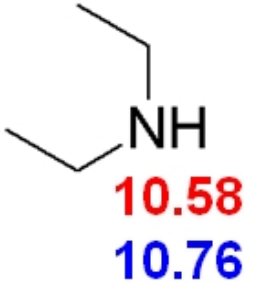

Fragment 1

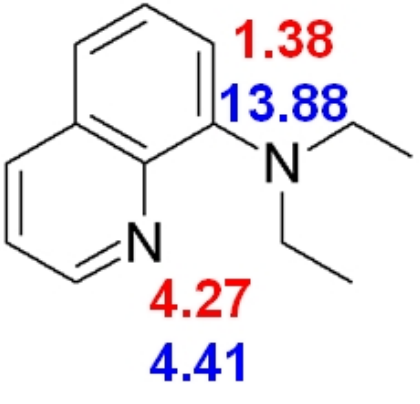

Fragment 2

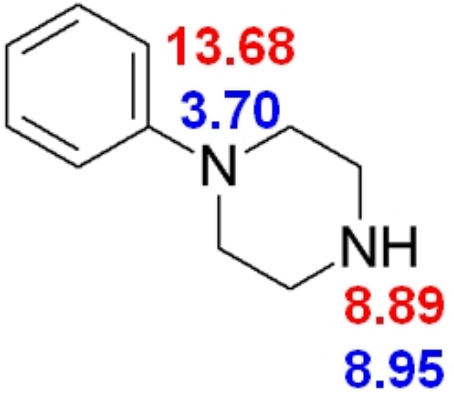

Fragment 3

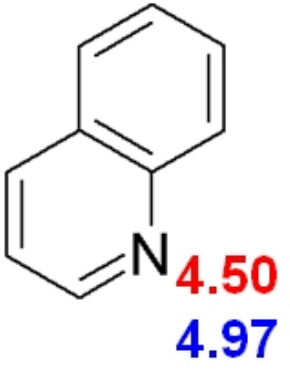

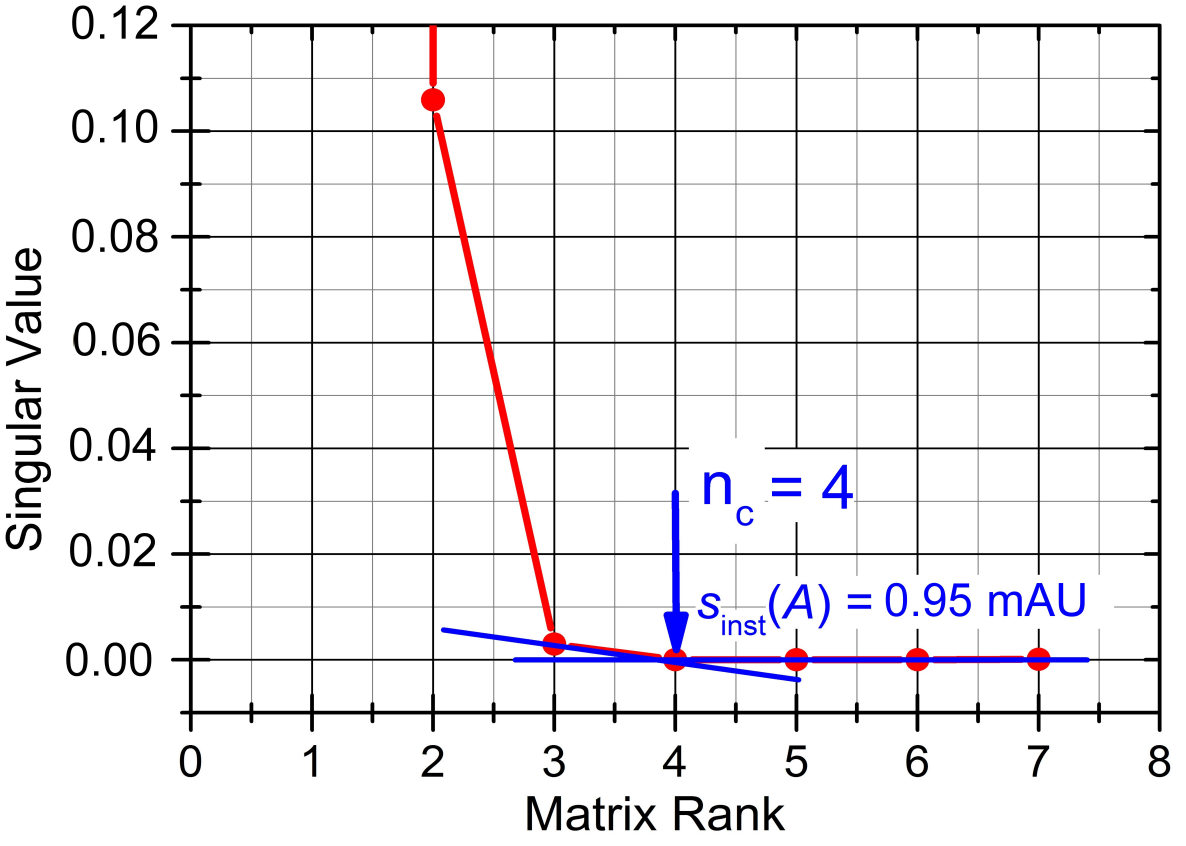
0.12
0.10
0.08
0.06
0.04
0.02
0.00
Singular Value
0
1
2
3
4
5
6
7
8
Matrix Rank
n_c = 4
s_inst(A) = 0.95 mAU

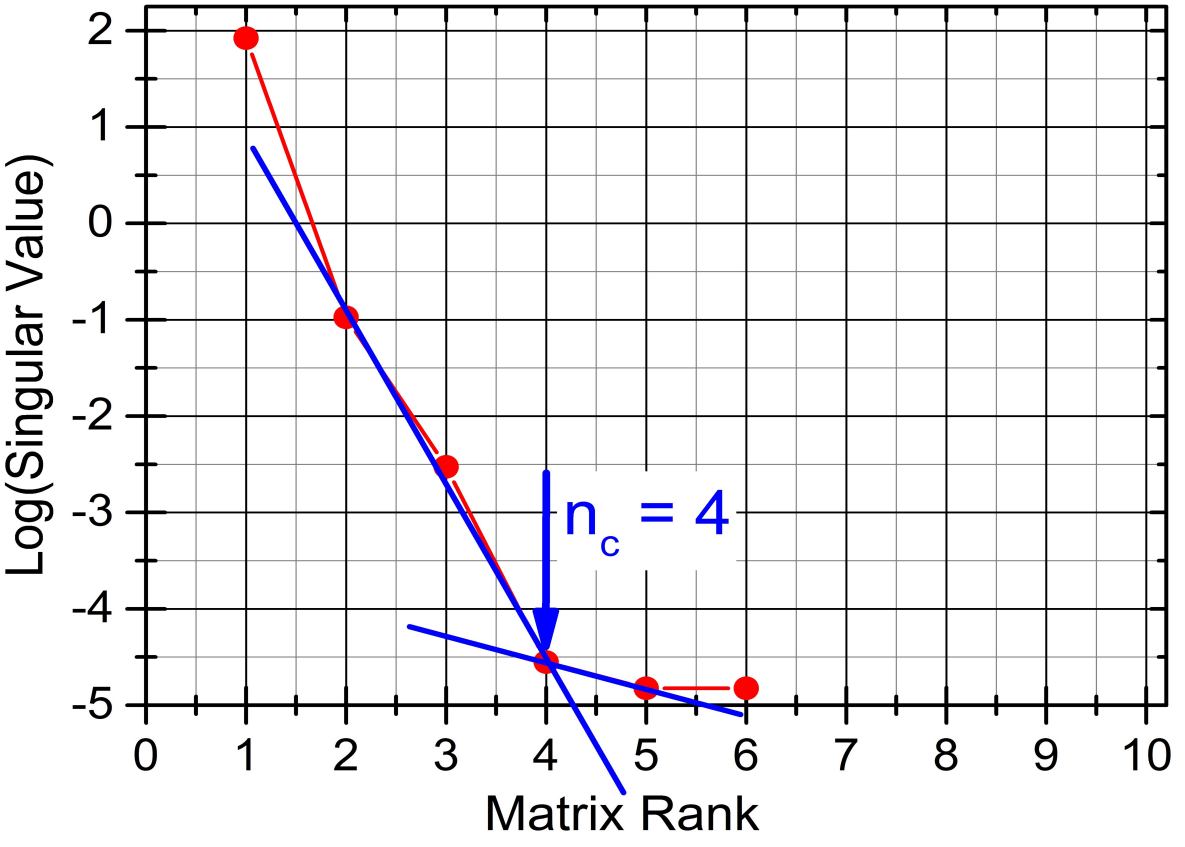
2
1
0
-1
-2
-3
-4
-5
Log(Singular Value)
0
1
2
3
4
5
6
7
8
9
10
Matrix Rank
n_c = 4

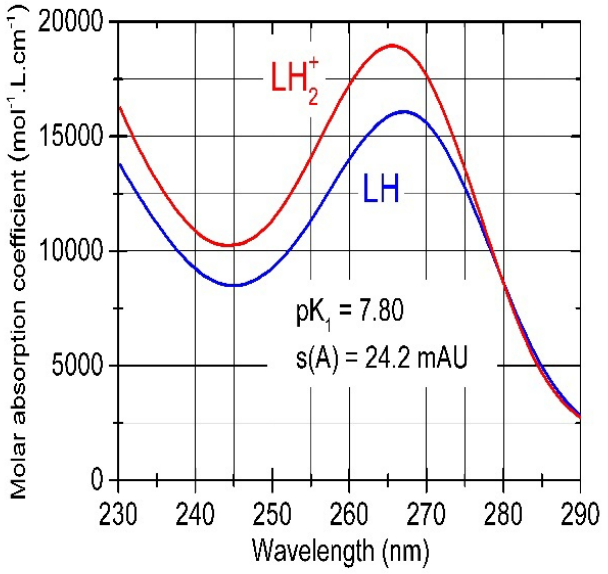
Molar absorption coefficient (mol^{-1}.L.cm^{-1})
Wavelength (nm)
LH_2^+
LH
pK_1 = 7.80
s(A) = 24.2 mAU

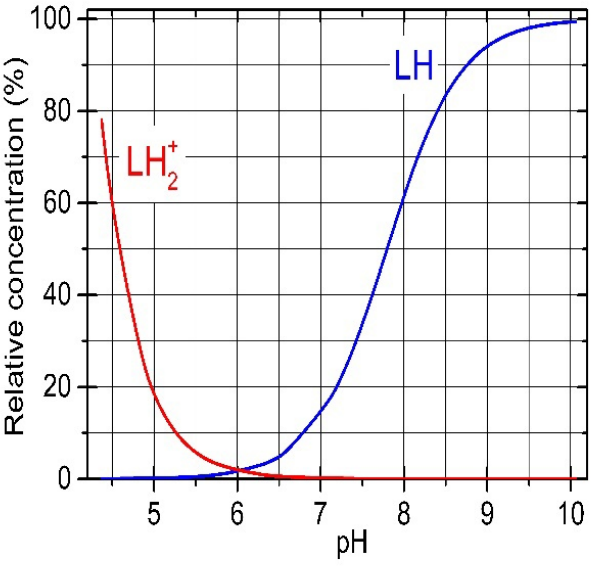
Relative concentration (%)
pH
LH
LH_2^+

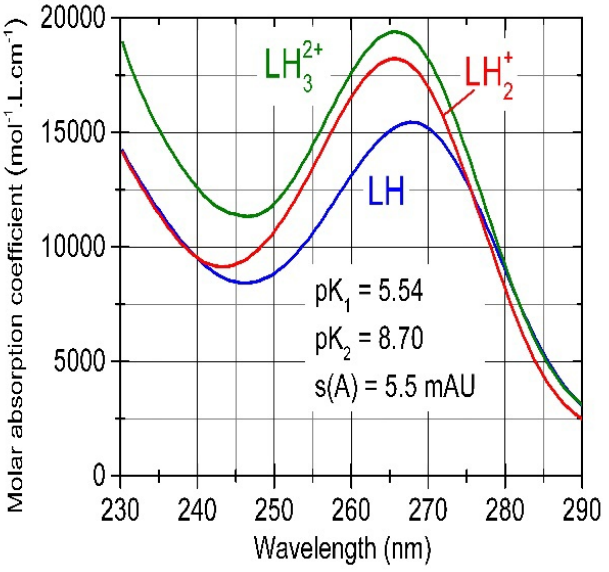
Molar absorption coefficient (mol^{-1}.L.cm^{-1})
Wavelength (nm)
LH_3^{2+}
LH_2^+
LH
pK_1 = 5.54
pK_2 = 8.70
s(A) = 5.5 mAU

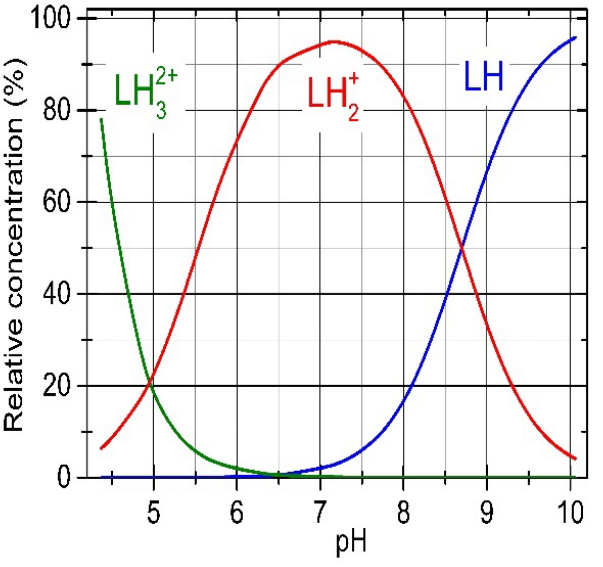
Relative concentration (%)
pH
LH_3^{2+}
LH_2^+
LH

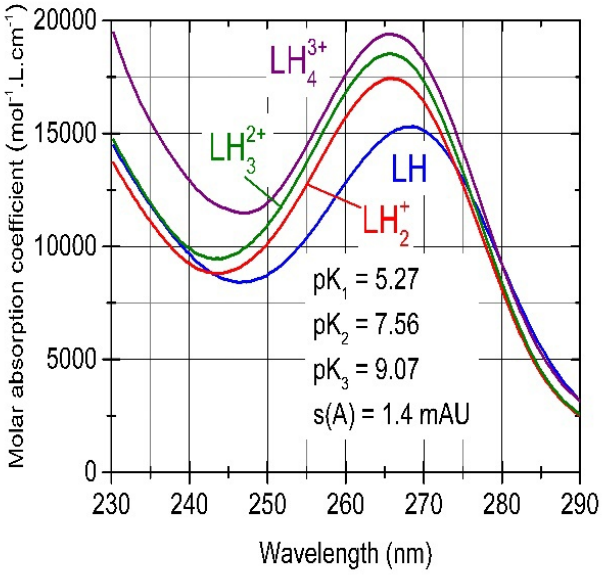
Molar absorption coefficient (mol^{-1}.L.cm^{-1})
Wavelength (nm)
LH_4^{3+}
LH_3^{2+}
LH
LH_2^+
pK_1 = 5.27
pK_2 = 7.56
pK_3 = 9.07
s(A) = 1.4 mAU

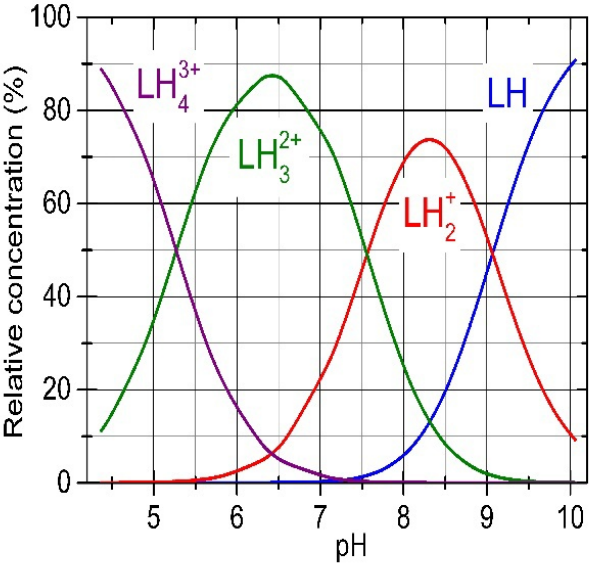
Relative concentration (%)
pH
LH_4^{3+}
LH_3^{2+}
LH_2^+
LH

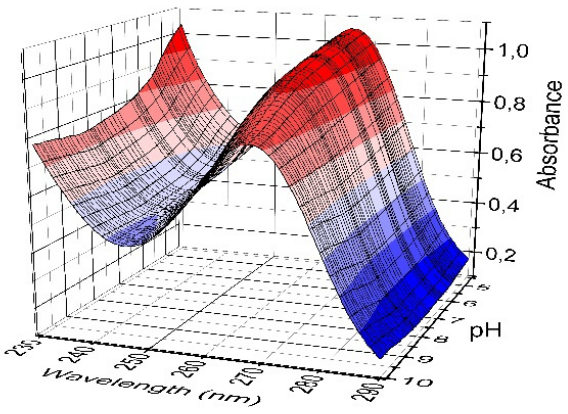
Absorbance
Wavelength (nm)
pH

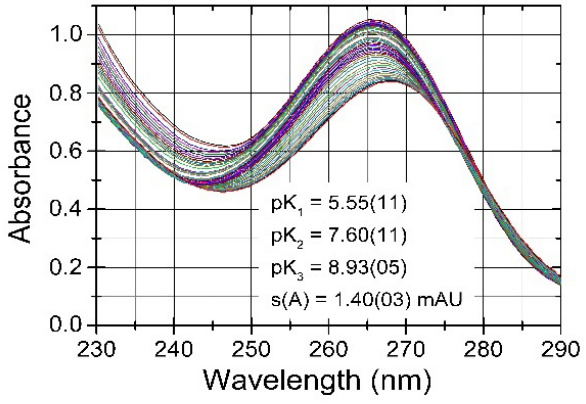
Absorbance
Wavelength (nm)
pK1 = 5.55(11)
pK2 = 7.60(11)
pK3 = 8.93(05)
s(A) = 1.40(03) mAU

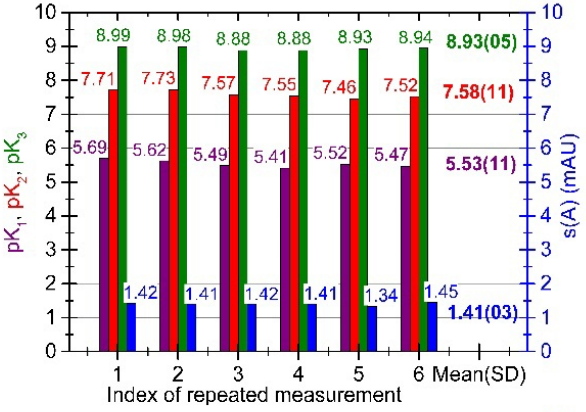
pK1, pK2, pK3
s(A) (mAU)
Index of repeated measurement
Mean(SD)
8.93(05)
7.58(11)
5.53(11)
1.41(03)

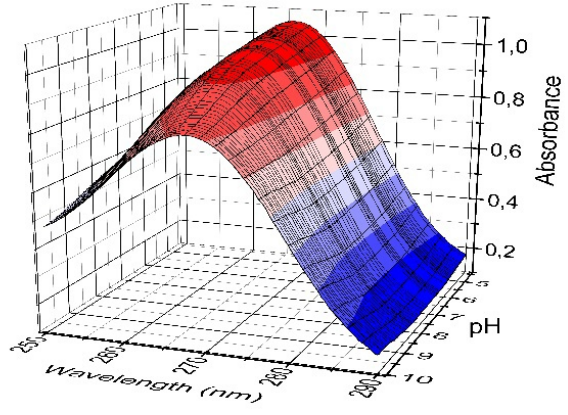
Absorbance
Wavelength (nm)
pH

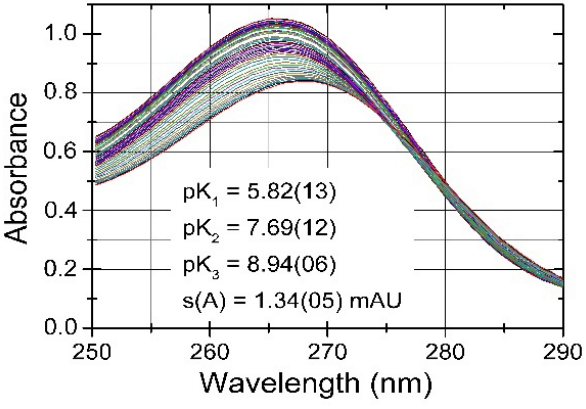
Absorbance
Wavelength (nm)
pK1 = 5.82(13)
pK2 = 7.69(12)
pK3 = 8.94(06)
s(A) = 1.34(05) mAU

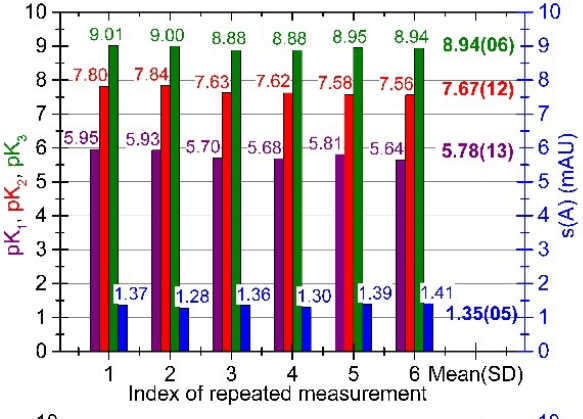
pK1, pK2, pK3
s(A) (mAU)
Index of repeated measurement
Mean(SD)
8.94(06)
7.67(12)
5.78(13)
1.35(05)

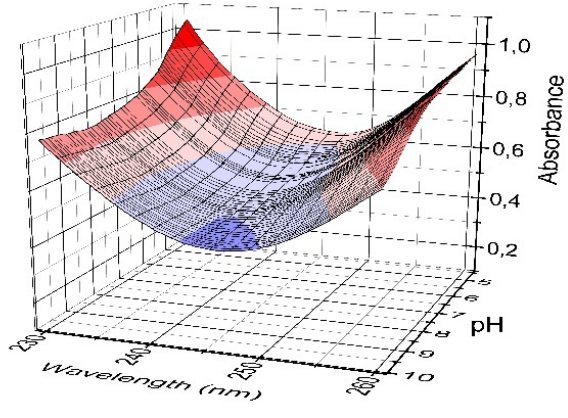
Absorbance
Wavelength (nm)
pH

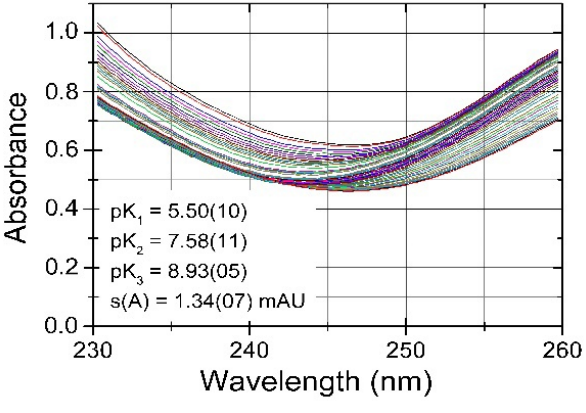
Absorbance
Wavelength (nm)
pK1 = 5.50(10)
pK2 = 7.58(11)
pK3 = 8.93(05)
s(A) = 1.34(07) mAU

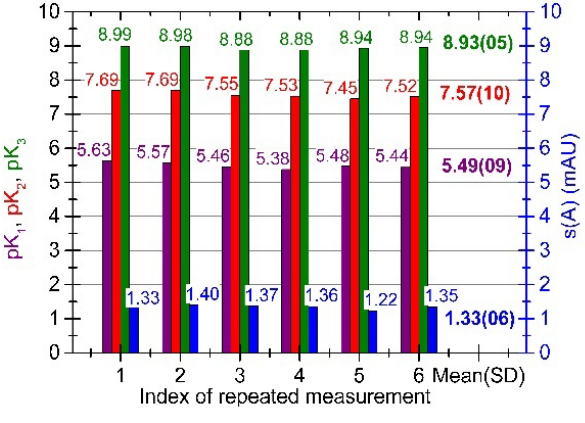
pK1, pK2, pK3
s(A) (mAU)
Index of repeated measurement
Mean(SD)
8.93(05)
7.57(10)
5.49(09)
1.33(06)

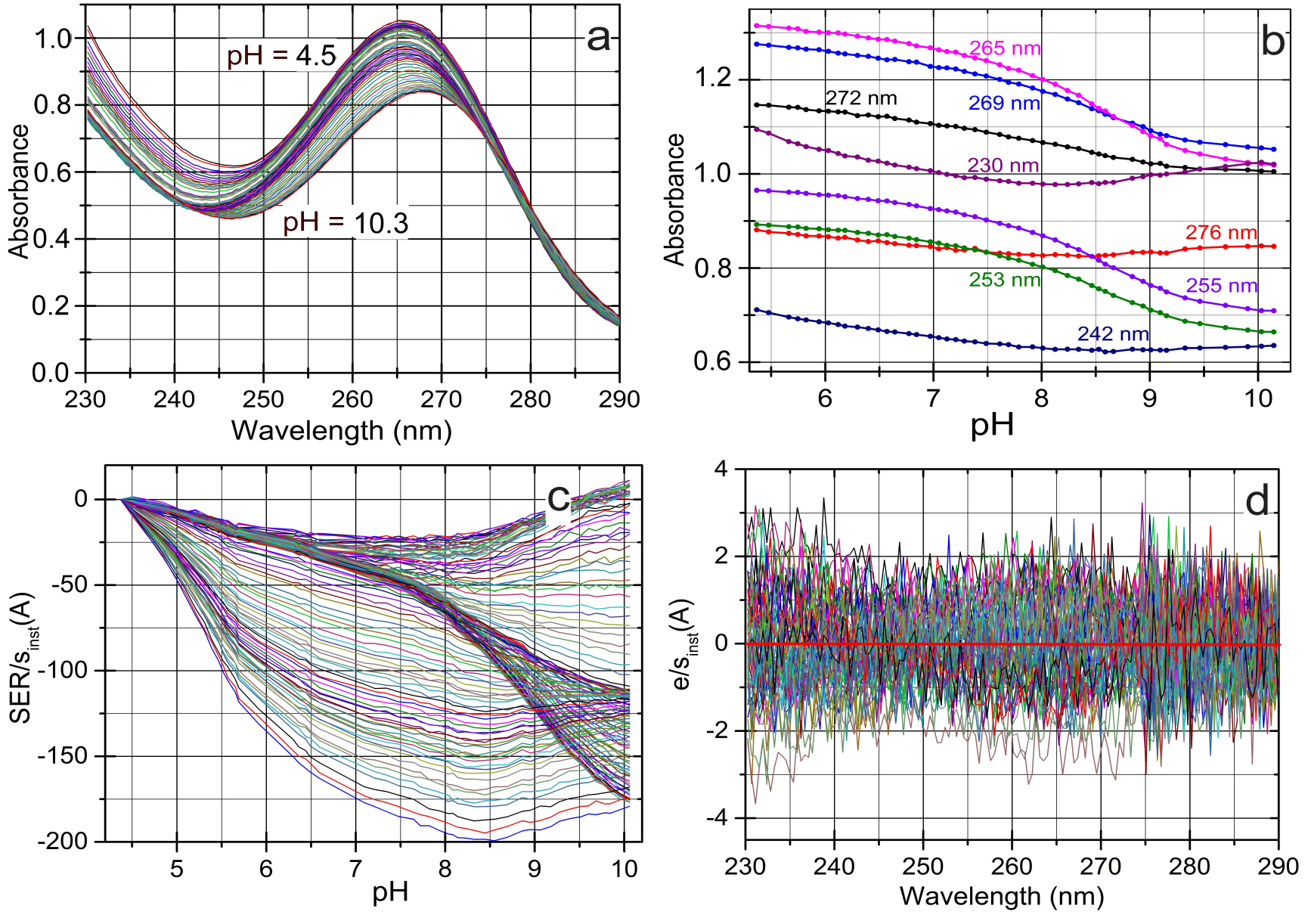
a
pH = 4.5
pH = 10.3
Absorbance
Wavelength (nm)
b
265 nm
269 nm
272 nm
230 nm
276 nm
253 nm
255 nm
242 nm
Absorbance
pH
c
SER/s_inst(A)
pH
d
e/s_inst(A)
Wavelength (nm)

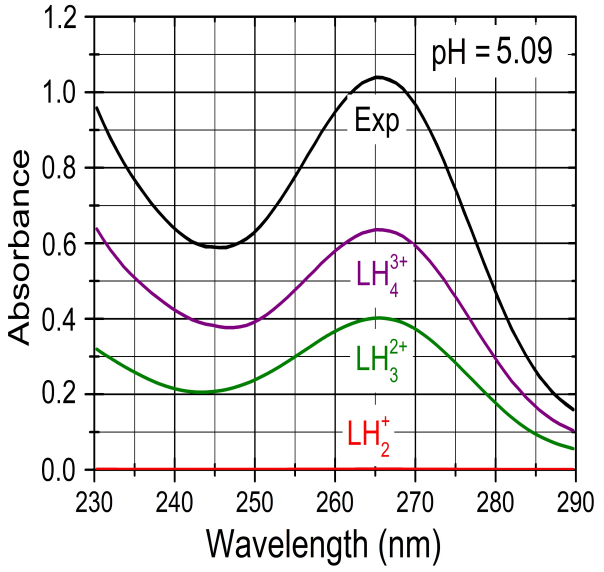
pH = 5.09
Exp
LH_4^{3+}
LH_3^{2+}
LH_2^+
Absorbance
Wavelength (nm)

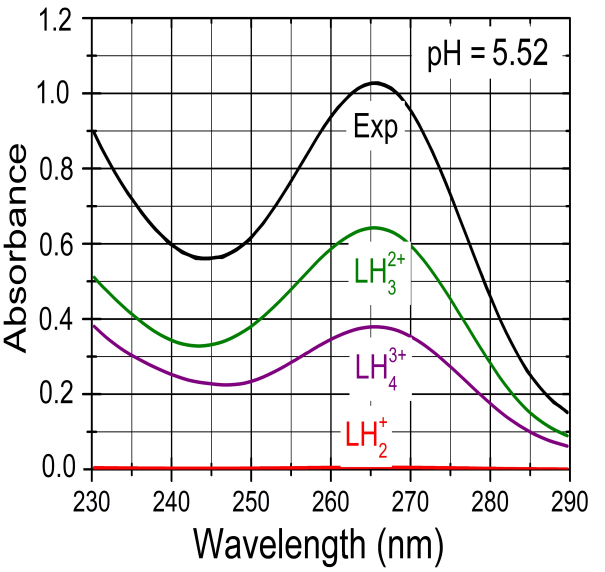
pH = 5.52
Exp
LH_3^{2+}
LH_4^{3+}
LH_2^+
Absorbance
Wavelength (nm)

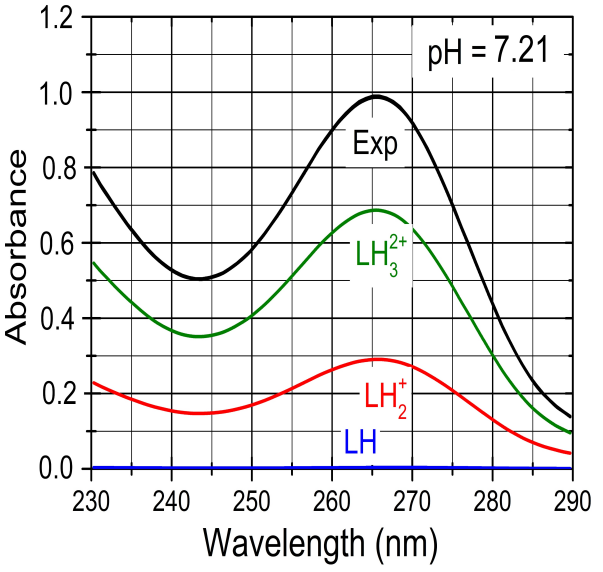
pH = 7.21
Exp
LH_3^{2+}
LH_2^+
LH
Absorbance
Wavelength (nm)

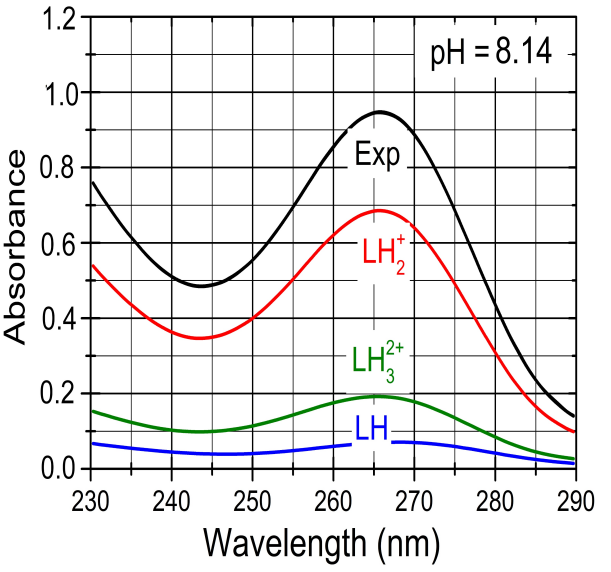
pH = 8.14
Exp
LH_2^+
LH_3^{2+}
LH
Absorbance
Wavelength (nm)

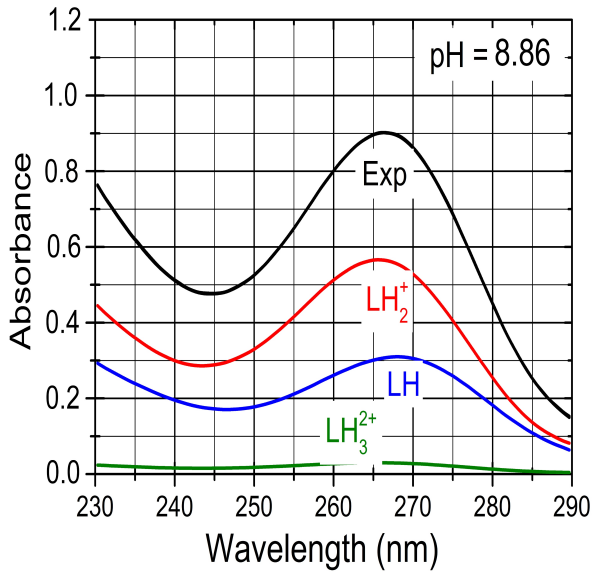
pH = 8.86
Exp
LH_2^+
LH
LH_3^{2+}
Absorbance
Wavelength (nm)

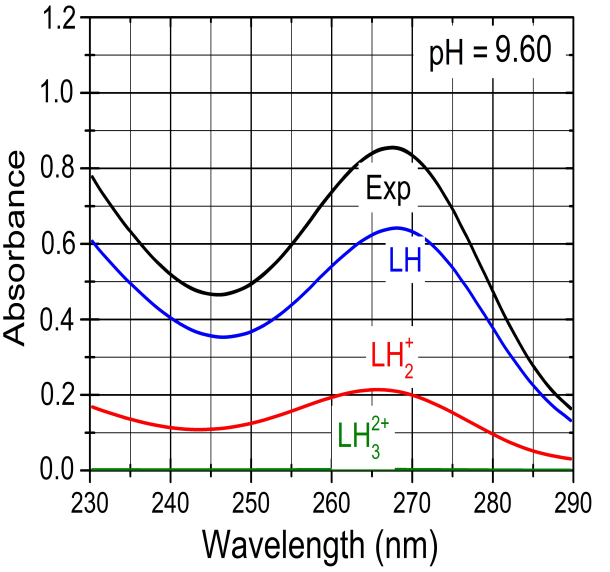
pH = 9.60
Exp
LH
LH_2^+
LH_3^{2+}
Absorbance
Wavelength (nm)

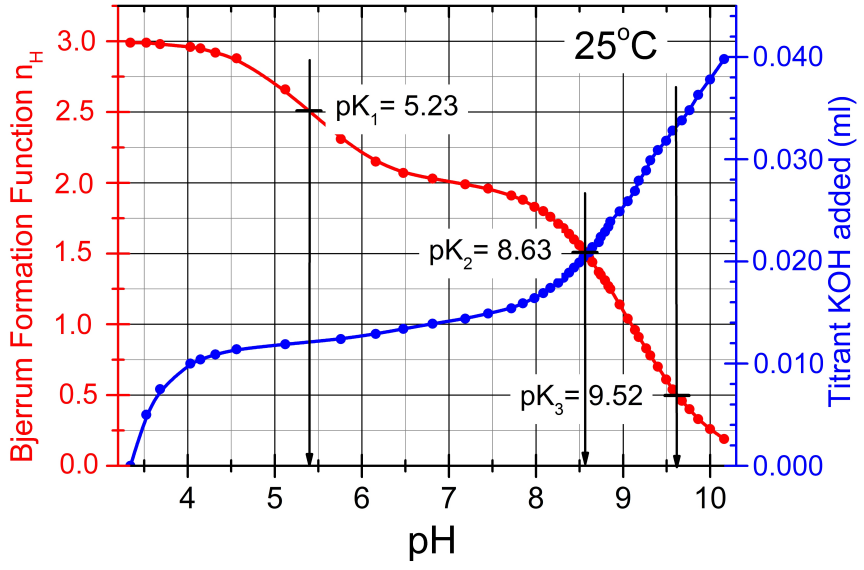
25°C
pK1= 5.23
pK2= 8.63
pK3= 9.52
Bjerrum Formation Function nH
Titrant KOH added (ml)
pH

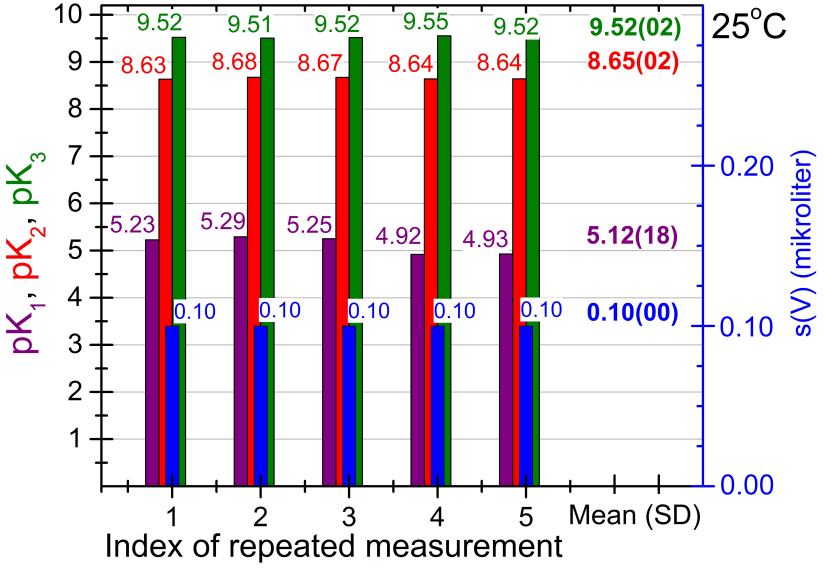
25°C
9.52 9.51 9.52 9.55 9.52 9.52(02)
8.63 8.68 8.67 8.64 8.64 8.65(02)
5.23 5.29 5.25 4.92 4.93 5.12(18)
0.10 0.10 0.10 0.10 0.10 0.10(00)
pK1, pK2, pK3
s(V) (mikroliter)
Mean (SD)
Index of repeated measurement

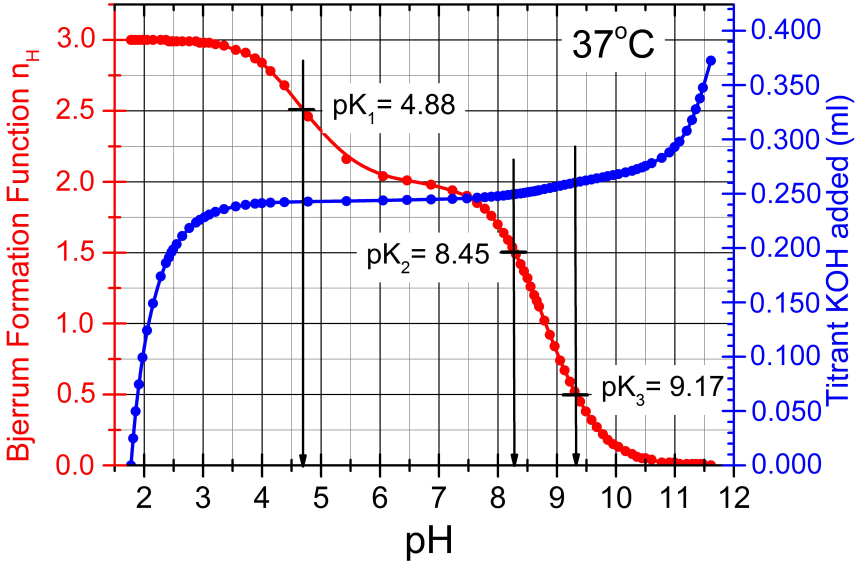
37°C
pK1= 4.88
pK2= 8.45
pK3= 9.17
Bjerrum Formation Function nH
Titrant KOH added (ml)
pH

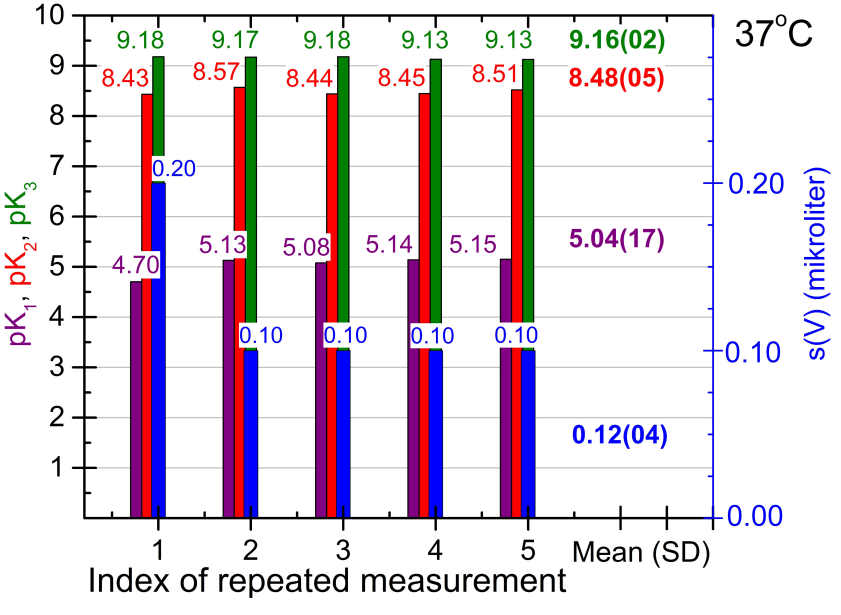
37°C
9.18 9.17 9.18 9.13 9.13 9.16(02)
8.43 8.57 8.44 8.45 8.51 8.48(05)
4.70 5.13 5.08 5.14 5.15 5.04(17)
0.20 0.10 0.10 0.10 0.10 0.12(04)
pK1, pK2, pK3
s(V) (mikroliter)
Mean (SD)
Index of repeated measurement

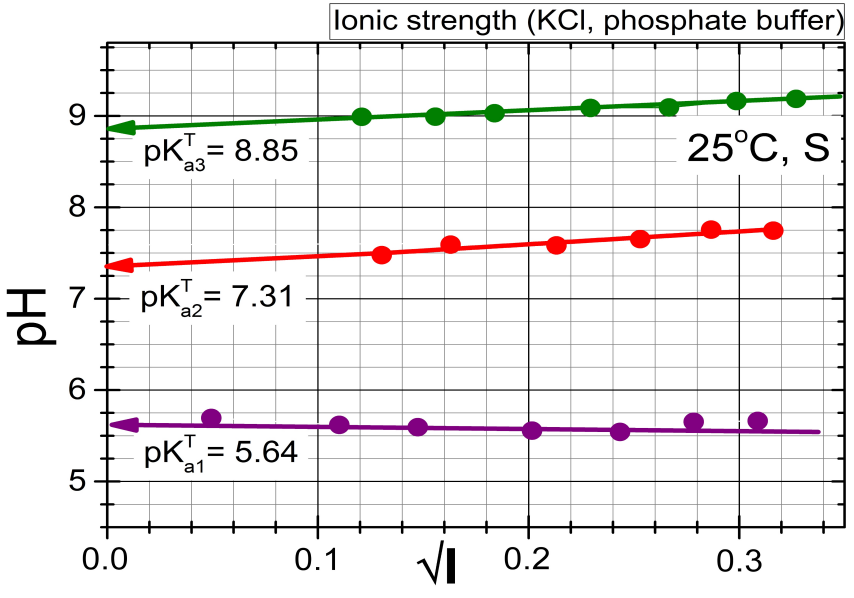
Ionic strength (KCl, phosphate buffer)
25°C, S
pK$_{a3}^{T}$= 8.85
pK$_{a2}^{T}$= 7.31
pK$_{a1}^{T}$= 5.64
pH
√I
0.0
0.1
0.2
0.3
5
6
7
8
9

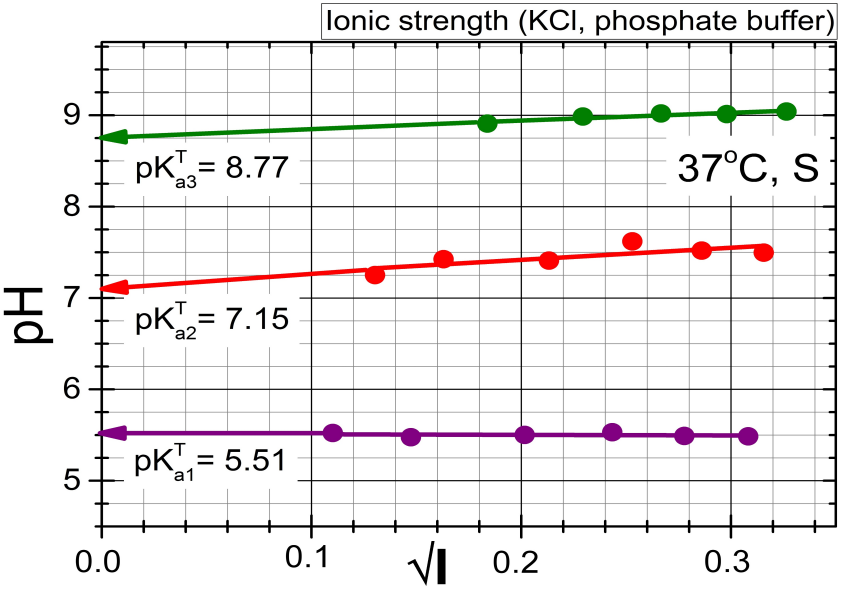
Ionic strength (KCl, phosphate buffer)
37°C, S
pK$_{a3}^{T}$= 8.77
pK$_{a2}^{T}$= 7.15
pK$_{a1}^{T}$= 5.51
pH
√I
0.0
0.1
0.2
0.3
5
6
7
8
9

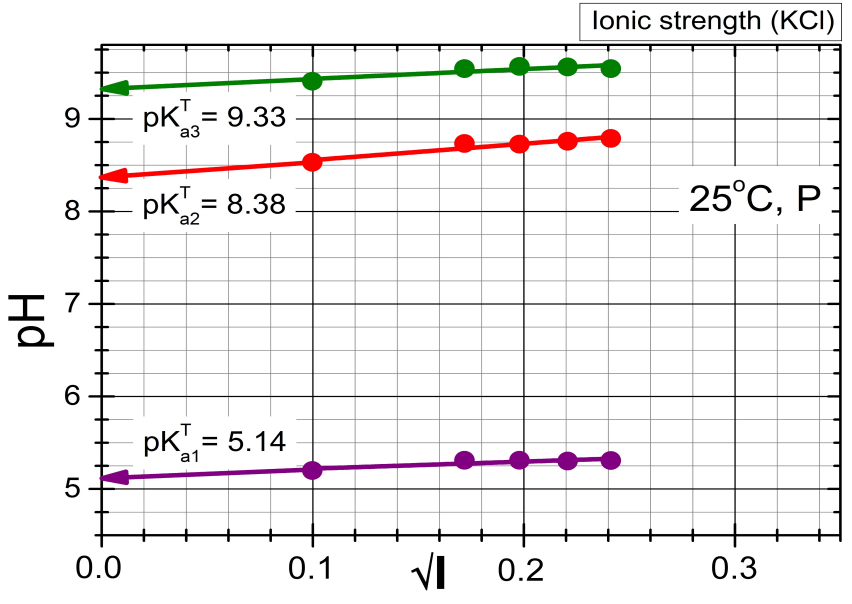
Ionic strength (KCl)
25°C, P
pK$_{a3}^{T}$= 9.33
pK$_{a2}^{T}$= 8.38
pK$_{a1}^{T}$= 5.14
pH
√I
0.0
0.1
0.2
0.3
5
6
7
8
9

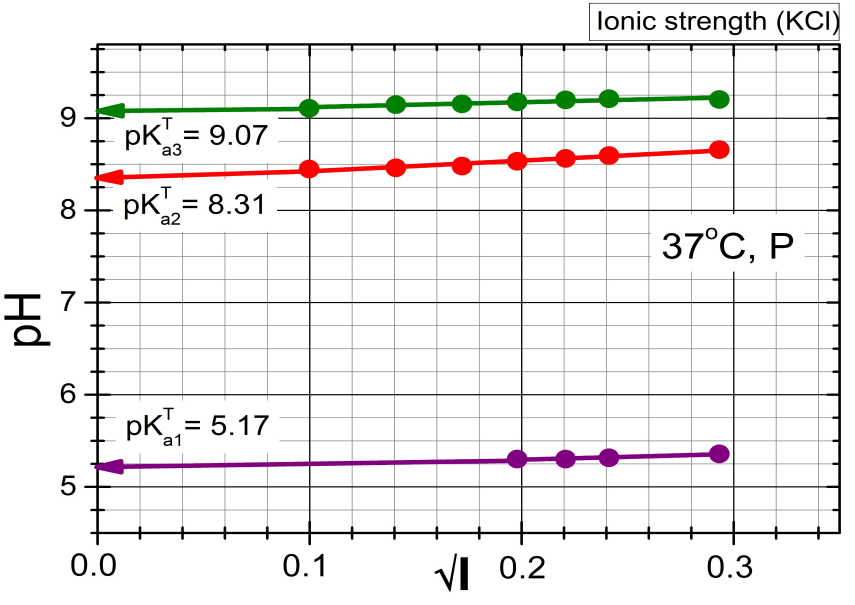
Ionic strength (KCl)
37°C, P
pK$_{a3}^{T}$= 9.07
pK$_{a2}^{T}$= 8.31
pK$_{a1}^{T}$= 5.17
pH
√I
0.0
0.1
0.2
0.3
5
6
7
8
9

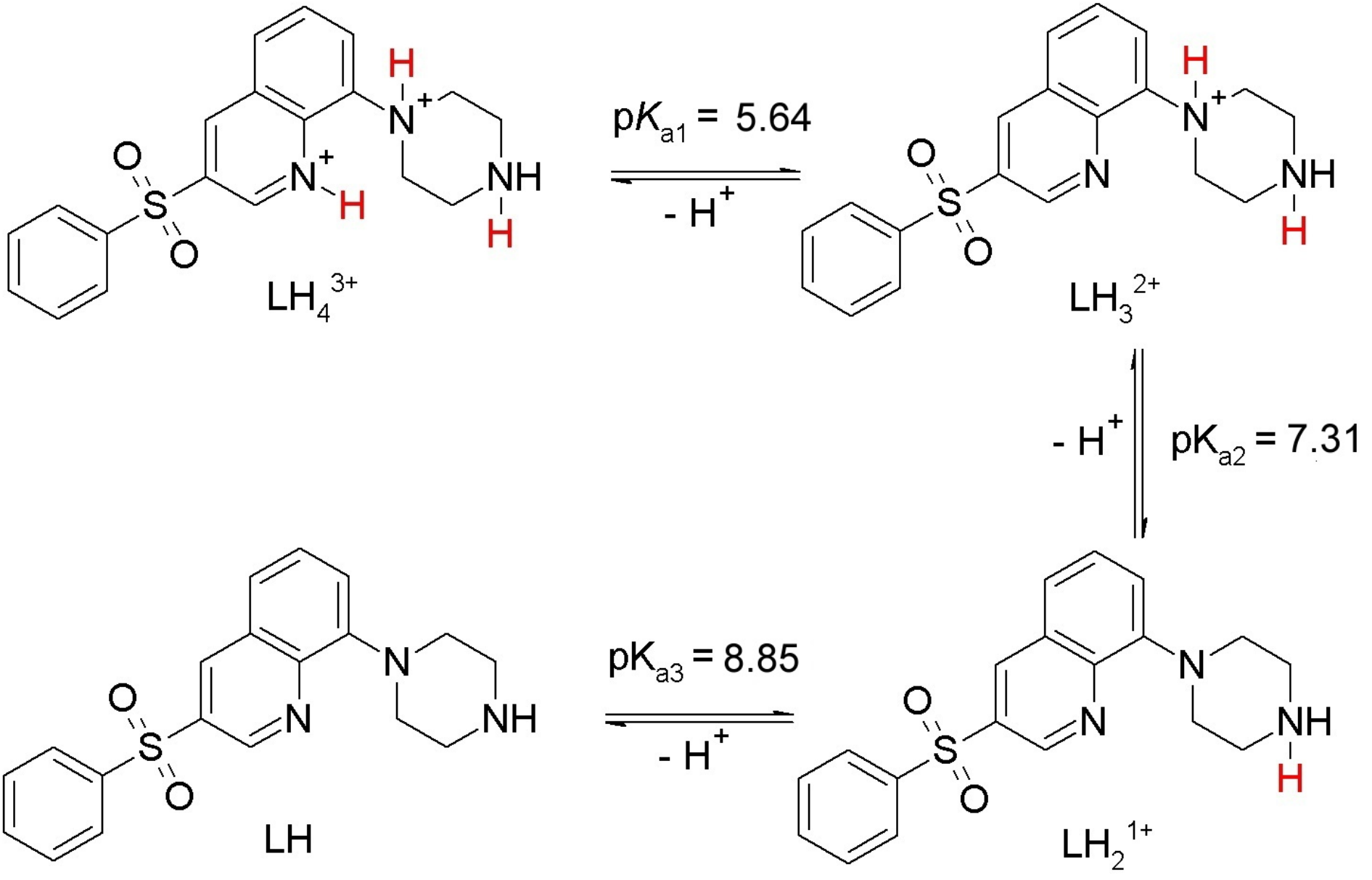
LH4 3+
pKa1 = 5.64
- H+
LH3 2+
- H+
pKa2 = 7.31
LH
pKa3 = 8.85
- H+
LH2 1+

Table 1 The regression refinement of three dissociation constants pK_{a1}, pK_{a2}, pK_{a3} of Intepirdine hydrochloride with SQUAD84 and REACTLAB at 25℃ and 37℃ in dependence on the ionic strength. Solution of 5.5 ×·10^{-5} M Intepirdine hydrochloride for n_s spectra measured at n_w wavelengths for n_z = 2 basic components L and H forms variously protonated species. The standard deviations of the parameter estimates are in the last valid digits in brackets. The resolution criterion and reliability of parameter estimates found are proven with goodness-of-fit statistics such as the residual standard deviation by factor analysis $s_k(A)$ [mAU], the mean residual $E\left|\bar{e}\right|$ [mAU], the standard deviation of absorbance after termination of the regression process $s(\hat{e})$ [mAU], the Sigma $s(A)$ [mAU] from REACTLAB and the Hamilton R-factor of relative fitness [%] from SQUAD84.

Temperature		**25°C**					**37°C**				
Ionic strength [mol/L]		0.0274	0.0463	0.0648	0.0829	0.1007	0.0274	0.0463	0.0648	0.0826	0.1004
Cattel´s scree plot indicating the rank of the absorbance matrix (INDICES)											
Number of spectra measured, n_s		53	55	53	51	54	51	54	55	51	46
Number of wavelengths, n_w		140	140	140	140	140	140	140	140	140	140
Number of light-absorbing species, k^*		4	4	4	4	4	4	4	4	4	4
Residual standard deviation, $s_k^*(A)$ [mAU]		1.41	1.16	1.27	1.27	1.26	1.16	1.16	1.23	1.17	1.18
Estimates of dissociation constants in the searched protonation model											
pK_{a1} (s_1), $LH_4^{3+} = H^+ + LH_3^{2+}$	SQUAD84	5.59(01)	5.53(01)	5.54(01)	5.65(01)	5.58(01)	5.47(01)	5.50(01)	5.53(01)	5.49(01)	5.49(01)
	REACTLAB	5.59(00)	5.56(01)	5.54(01)	5.65(01)	5.66(01)	5.48(01)	5.50(01)	5.53(01)	5.49(00)	5.49(01)
pK_{a2} (s_2), $LH_3^{2+} = H^+ + LH_2^+$	SQUAD84	7.59(01)	7.56(01)	7.65(01)	7.75(01)	7.71(01)	7.42(01)	7.41(01)	7.62(01)	7.52(01)	7.50(01)
	REACTLAB	7.59(00)	7.58(01)	7.65(00)	7.76(00)	7.74(00)	7.42(00)	7.41(00)	7.62(00)	7.52(00)	7.50(00)
pK_{a3} (s_3), $LH_2^+ = H^+ + LH$	SQUAD84	9.03(00)	9.08(00)	9.09(00)	9.16(00)	9.17(00)	8.91(00)	8.99(00)	9.02(00)	9.01(00)	9.04(00)
	REACTLAB	9.03(00)	9.09(00)	9.09(00)	9.16(00)	9.19(00)	8.91(00)	8.99(00)	9.02(00)	9.01(00)	9.04(00)
Goodness-of-fit test with the statistical analysis of residuals											
Mean residual $E\left|\bar{e}\right|$ [mAU]	SQUAD84	1.08	0.87	0.94	0.96	0.96	0.88	0.89	0.94	0.90	0.90
	REACTLAB	1.09	0.87	0.95	0.98	0.97	0.90	0.91	0.96	0.92	0.92
Standard deviation of residuals $s(\hat{e})$ [mAU]	SQUAD84	1.41	1.16	1.24	1.27	1.26	1.16	1.17	1.23	1.17	1.18
	REACTLAB	1.39	1.13	1.22	1.25	1.24	1.14	1.15	1.21	1.16	1.16
Sigma from ReactLab [mAU]	REACTLAB	1.41	1.14	1.23	1.26	1.25	1.15	1.17	1.22	1.18	1.17
Hamilton R-factor from SQUAD84 [%]	SQUAD84	0.17	0.15	0.17	0.17	0.15	0.17	0.14	0.15	0.16	0.16

Table 2. ESAB regression refinement of common and group parameters for a pH-metric titration of Intepirdine hydrochloride titrated with HCl and KOH: the estimated dissociation constants pK_{a1}, pK_{a2}, pK_{a3} of Intepirdine hydrochloride when their standard deviations in last valid digits are in parentheses. The reliability of parameter estimation is proven with a goodness-of-fit statistics: the arithmetic mean of residuals $E(\hat{e})$ [mL], the mean of absolute value of residuals, $E|\hat{e}|$ [mL], the standard deviation of residuals $s(\hat{e})$ [mL], the residual skewness $g_1(\hat{e})$ and the residual kurtosis $g_2(\hat{e})$ proving a Gaussian distribution and Jarque-Berra normality test.
Common parameters refined: pK_{a1}, pK_{a2}, pK_{a3}. ***Group parameters refined****: H_0, H_T, L_0.* ***Constants:*** t = 25.0 °C, pK_w = 13.9799, $s(V) = s_{inst}(V)$ = 0.0001 mL, I_0 adjusted (in vessel), I_T = 0.8138 (in burette KOH) or 1.0442 (in burette HCl).

Temperature	**25°C**					**37°C**				
Ionic strength I_0 [mol/L]	0.0099	0.0295	0.0392	0.0488	0.0582	0.0295	0.0392	0.0487	0.0582	0.0860
Estimates of the group parameters H_0, H_T and L_0 in the searched protonation model										
Number of points used *n*	23	30	31	34	36	38	35	35	37	37
H_0 × 1E+04 [mol/L]	1.56(05)	1.60(02)	1.91(04)	1.88(03)	1.72(02)	2.09(03)	2.07(04)	2.09(03)	1.89(04)	2.27(03)
H_T [mol/L]	0.8138	0.8138	0.8138	0.8138	0.8138	0.8138	0.8138	0.8138	0.8138	0.8138
L_0 × 1E+04 [mol/L]	4.45(03)	4.41(01)	4.38(02)	4.31(02)	4.09(01)	3.86(02)	3.92(02)	3.78(01)	3.77(02)	3.53(02)
Estimates of the common parameters *i.e.* dissociation constants in the searched protonation model										
pK_{a1}	5.20(03)	5.31(03)	5.31(03)	5.30(04)	5.31(06)	5.01(05)	5.08(05)	5.30(04)	5.32(04)	5.36(04)
pK_{a2}	8.53(01)	8.73(01)	8.73(01)	8.76(01)	8.79(01)	8.48(01)	8.52(01)	8.56(01)	8.59(01)	8.66(01)
pK_{a3}	9.41(01)	9.54(01)	9.54(01)	9.56(01)	9.54(01)	9.16(01)	9.16(01)	9.20(01)	9.21(01)	9.20(01)
Goodness-of-fit test with the statistical analysis of residuals										
Bias, arithmetic mean of residuals $E(\hat{e})$, [mL]	-4.35E-06	-1.33E-05	-1.31E-21	-5.59E-05	-1.51E-21	2.63E-06	-2.86E-05	-2.00E-05	-1.35E-05	-1.89E-05
Mean of absolute value of residuals, $E\|\hat{e}\|$, [mL]	0.00013	0.00007	0.00011	0.00011	0.00007	0.000	0.00014	0.00013	0.00014	0.00013
Residual standard deviation, $s(\hat{e})$, [mL]	0.00016	0.00009	0.00018	0.00014	0.00011	0.00016	0.00017	0.00017	0.00017	0.00015
Residual skewness $g_1(\hat{e})$	0.07	-0.25	-0.21	-0.39	0.28	-0.70	-0.14	-0.09	-0.18	-0.06
Residual kurtosis $g_2(\hat{e})$	1.98	2,05	2.26	1.82	3.60	4.15	2.24	2.30	2.08	2.10
Jarque-Berra test of residuals normality: *p*,	0.955, Accepted	0.752, Accepted	0.795, Accepted	0.498, Accepted	0.660, Accepted	0.164, Accepted	0.888, Accepted	0.928, Accepted	0.928, Accepted	0.957, Accepted